

AD-A059 034

CASE WESTERN RESERVE UNIV CLEVELAND OHIO SCHOOL OF EN--ETC F/8 14/2
THEORY AND CONSTRUCTION OF TIME RESOLVED X-RAY SPECTROMETER.(U)

AUG 78 O K MAWARDI, C SPECK, R VESEL

AFOSR-75-2806

UNCLASSIFIED

AFOSR-TR-78-1269

NL

OF
AD
A059034



AD A059034

DDC FILE COPY

(18) AFOSR TR- 78-1269 (19)

(2)

LEVEL II

CASE WESTERN RESERVE UNIVERSITY

School of Engineering

(6) THEORY AND CONSTRUCTION OF
TIME RESOLVED X-RAY SPECTROMETER

(9) FINAL TECHNICAL REPORT #34 Jan 75-31 Jan 78
January 31, 1975 to January 31, 1978

(16) 2301

(17) A2
to

(12) 93 p.

Air Force Office of Scientific Research
for Grant No. AFOSR-75-2806

(15)

DDC
RECEIVED
SEP 25 1978
B

(10) O.K. / Mawardi, C. / Speck, R. / Vesel A. / Ferendeci
Case Western Reserve University
Cleveland, Ohio

(11) August 1978
DISTRIBUTION STATEMENT A

Approved for public release;
Distribution Unlimited

* Prepared for the Air Force Office of Scientific Research. Approved for public release; distribution unlimited, reproduction in whole or in part is permitted for any purpose of the United States Government.

AIR FORCE OFFICE OF SCIENTIFIC RESEARCH (AFSC)
NOTICE OF TRANSMITTAL TO DDC
This technical report has been reviewed and is
approved for public release IAW AFR 190-12 (7b).
Distribution is unlimited.
A. D. BLOSE
Technical Information Officer

403 474

set

TABLE OF CONTENTS

Introduction	i
PART I	
Development of a Time-Resolved X-Ray Spectrometer for Intense X-Ray Sources	I
Research Summary	I:1
Introduction	I:1
The X-Ray Spectrometer: Design Considerations	I:2
Physical Structure	I:7
Exploding Wire X-Ray Source	I:8
References	I:10
PART II	
A Preliminary Design of a Nanosecond Resolution X-Ray Detector for an X-Ray Spectrometer	II
Introduction	II:1
1.1 A Basic X-Ray Spectrometer System	II:1
1.2 Purpose of the Thesis	II:4
The X-Ray Sources	II:7
2.1 The Exploding Wire	II:7
2.2 Characterization of the X-Ray Pulse	II:10
The Curved Crystal Spectrometer	II:22
3.1 Characteristics of the Spectrometer	II:22
3.2 Sensitivity of the Spectrometer	II:24
3.3 Tests Performed on the Spectrometer	II:26
High Sensitivity Vidicon Camera	II:29
4.1 Requirements of the Detector	II:29
4.2 Electronics for the Camera Head	II:30
4.3 Optics for the Detector	II:41
The Detection System	II:44
Tests and Results	II:46

UNANNOUNCED JUSTIFICATION		
BY		
DISTRIBUTION/AVAILABILITY CODES		
Dist.	AVAIL	and/or SPECIAL
A		

6.1 Introduction	II:46
6.2 Steady State Testing	II:46
6.3 Pulsed Testing	II:48
6.4 Integrating and Storage Mode Operation	II:55
Conclusions and Work to be Done	II:57
7.1 Conclusions Based on Literature Search	II:57
7.2 Work to be Done	II:58
References	II:61
Appendix 1	II:63
Appendix 2	II:64
Appendix 3	II:66
Appendix 4	II:67

PART III

Plasma Injection for a SHIVA MachineIII:1
IntroductionIII:1
Criteria for Plasma DensitiesIII:1
Summary of Diagnostics PerformedIII:2
ResultsIII:3
ReferencesIII:4

SEARCHED	INDEXED
SERIALIZED	FILED
OCT 1964	
FBI - NEW YORK	
A	

Introduction

This final report for the period January 31, 1975 to January 31, 1978 describes the summary findings of three projects all successfully completed during this time.

The first part of the report concentrated on the development of an X-ray time resolved spectrometer capable of analyzing spectra in the energy range of 4.2 KeV to 12.4 KeV. The spectrometer which had a time resolution of approximately 2.4 μ sec. with a wave length discrimination of better than 4% is described in detail in Part I of this report.

The second section of this report concentrates on the associated electronics for the detection of the optical signal which appears at the plastic scintillator attached on the X-ray spectrometer. Originally we had considered the use of a Kerr cell camera to record the output from the scintillator. We found it more expedient instead to use a video storage system to detect and store the signal from the spectrometer. The unfolding of the X-ray spectrum can be performed at a much slower rate. The details of the detection accessories are included in Part II of this report.

Finally, the report concludes with the description and main findings of an attempt to use a plasma gun to inject plasma in the implosion chamber of a SHIVA experiment. The original plan was to provide a total injection mass of 1 mgm. As it turns out, a much higher mass could be injected. The outcome of our investigations appears to be most promising and the details of the work are described in Part III of this report.

This final report for the period January 31, 1975 to January 31, 1976 describes the summary findings of three projects still successfully completed during this time. The first part of the report concentrated on the development of an X-ray time resolved spectrometer capable of analyzing spectra in the energy range of 10 to 100 keV. The second section of this report concentrated on the associated electronics for the detector of the optical signal which appears as the elastic scattering intensity in the X-ray spectrometer. Originally we had considered the use of a Kerr cell camera to record the output from the spectrometer. We found it more expedient instead to use a video storage system to detect and store the signal from the spectrometer. The unfolding of the X-ray spectrum can be performed at a much slower rate. The details of the detector spectrometer are included in Part II of this report.

PART I

**DEVELOPMENT OF A TIME-RESOLVED X-RAY SPECTROMETER FOR
INTENSE X-RAY SOURCES**

by

CARLTON E. SPECK

Part II, the second concludes with the description and main findings of an attempt to use a plasma jet to inject plasma in the ionization chamber of a SHIVA experiment. The original plan was to produce a total injection mass of 1 mg. It is found that 3 mg of higher mass could be injected. The outcome of our investigations appears to be most promising and the details of the work are described in Part III of this report.

Research Summary

During the contract period an x-ray spectrometer has been designed and constructed which is capable of analyzing spectra in the energy range of 4.2 keV to 12.4 keV or correspondingly in the wavelength range of 1\AA to 3\AA . The spectrometer can time resolve the observed spectra to approximately 2.4nsec with a wavelength resolution better than 4%. Concurrent with the development of the spectrometer has been the design and construction of a flash x-ray source. This source is in the form of an exploding wire device. Presently tungsten wires are utilized with driving voltages up to about 15 keV. This device is a prolific source of x-rays in the range of the spectrometer with emission times over several hundred nsec.

Introduction

The renewed interest in the development of exploding wire and foil devices as intense sources of x-rays has necessitated the development of new diagnostic techniques capable of time resolving x-ray spectra within a total emission time on the order of a hundred nanoseconds. In the work reported here such a time-resolved x-ray spectrometer has been developed based on the convex curved crystal geometry of Birks⁽¹⁾ (See Fig. 1). In this geometry the collimated x-ray beam to be analyzed is incident on a bent diffracting crystal such that the Bragg condition is satisfied for photons of different energies at different locations along the crystal. In this manner a wide energy range of x-ray photons can be simultaneously diffracted. Using a plastic scintillator at the output of the spectrometer provides a means of converting the x-rays to visible photons. The visible image can then be resolved in time by using existing high-speed devices such as an electronic smear or Kerr cell camera.

In order to have a suitable flash x-ray source, an exploding wire facility has also been developed under this contract. The basic apparatus is similar to that reported by Händel⁽²⁾ but has been designed to be compatible with the capacitor bank and high voltage insulator system used in an existing plasma focus device.

The development of the x-ray spectrometer and the exploding wire apparatus are detailed in the remainder of this report.

The X-Ray Spectrometer

Design Considerations

Only limited data has been reported in the literature concerning the characteristics of the x-radiation from exploding wire x-ray sources. For initial design purposes the observations of Händel et al.⁽³⁾ have been utilized. Their observations indicated that significant amount of hard x-rays were emitted at energies comparable to the driving voltage (a 20 kV capacitor bank voltage in their experiments) when tungsten wires were exploded. The emission occurred as a single pulse in time with a half-amplitude width of about 30 nsec. Collimated scintillator/photomultiplier observations and time-integrated pin-hole camera pictures located the source of the most intense hard x-ray emission to be a small circular area surrounding the wire on the anode face although x-rays were also emitted from the body of the wire near its anode end. They suggested that the hard x-rays were produced as if the device were an x-ray tube with the electron beam being provided by thermionic emission from the wire while the observed softer x-radiation from the body of the wire was attributed to Bremsstrahlung.

Based on these observations it was decided to limit the maximum energy of

the spectrometer to a value somewhat lower than 20keV. This decision resulted in two design simplifications. First, the development of the x-ray source was more rapid since an existing 20 keV capacitor bank could be employed. Second, the detection of x-rays on nanosecond time scales suggested the use of a fast plastic scintillator at the output plane of the spectrometer. This material would have to be excessively thick if detection of x-rays above about 15keV were attempted. The latter will be discussed more fully below.

Conversion of x-rays to visible photons on nanosecond time scales is effectively performed in a plastic scintillator. Commercially available material such as NE102 (Nuclear Enterprises, Inc.) has decay times and therefore time resolutions on the order of 2.4nsec. For simplicity in the design of the optics between the scintillator and the detector used to observe the visible photons, it was decided to use a flat output plane rather than a circular one as is common in high resolution spectrometers. Since x-rays which diffract off the analyzing crystal will not all pass normal to the surface of the scintillator when it is in the form of a flat sheet, it is necessary to keep the detector thin. If it is too thick, the x-rays which pass obliquely through the sheet increase the length along the scintillator which is excited and therefore the resolution of the spectrometer will be degraded.

The required thickness of the scintillator material is a function of the energy dependent absorption characteristics of the material. Although absorption efficiencies are not available from the manufacturer for x-ray energies below 20 keV, they can be inferred from the measurements of Berstein.⁽⁴⁾

Assuming the absorption goes as

$$A = 1 - e^{-\mu d}$$

where μ is the photoelectric absorption coefficient of the scintillator, and d is its thickness, Bernstein's data for NE102 material fitted at 5.1keV and $d = 2 \times 10^{-2}$ cm yields

$$\mu = \frac{2.37 \times 10^3}{E^3}$$

where E is the x-ray energy in keV. In fitting this data it has been assumed that $\mu \propto E^{-3}$ consistent with the photoelectric effect. Using this expression, a calculation of the thickness at which $1/e$ of the x-rays will be absorbed yields the following values:

E (keV)	d (cm)	d (mil)
20	1.55	610
15	0.65	256
10	0.19	75
5	0.02	7.9

Since some of the x-rays will pass through the scintillator with an angle of 45° (See Fig. (1) with the curved sheet replaced by a flat one), the spatial resolution along the sheet at these energies will be on the order of thickness of the detector. In attempting to keep the resolution of the spectrometer relatively high, a value of 30 mil was chosen for the thickness. This insures that the resolution is dependent upon the collimation system rather than the scintillator. From the above thickness calculations it is noted that this will limit the high energy absorption, say above 10keV, but is entirely adequate at the lower energies.

The actual conversion efficiency at the higher x-ray energies is not as poor as might be inferred from the above observations. Approximately 500eV of absorbed x-ray energy is required to produce one 3eV visible photon. Hence, although fewer high energy x-rays are absorbed, each one which is absorbed delivers a proportionally greater amount of energy to the scintillator. For

30 mil thick NE102 material and assuming a value of approximately $2E$ visible photons for each absorbed x-ray of energy E keV , the following percentage absorption and relative conversion efficiencies result:

E (keV)	A (%)	η
20	2%	0.8
15	5%	1.5
10	17%	3.4
5	76%	7.6

where η is defined as the relative number of visible photons produced times A . Clearly, with the present scintillator, the spectrometer is most sensitive in the energy range below about 15keV.

At the low energy end of the spectrum the sensitivity is limited by any absorber in the path of the x-ray beam. Using an exploding wire for the source it is necessary to place a window which is opaque to visible light at the entrance to the spectrometer. These sources also produce an intense flash of visible light which would scatter inside the spectrometer and ultimately would be detected along with the photons produced in the scintillator. The window also serves the purpose of preventing the vaporized wire from entering the spectrometer and subsequently plating out the diffraction crystal.

The lowest density material which can be obtained in thin pin-hole free self-supporting sheets is beryllium. Mass absorption characteristics of Be are readily available in the literature.⁽⁵⁾ Since 5 mil Be sheet is available off the shelf and is capable of supporting a vacuum over reasonable spans, it was chosen as the window material. The absorption characteristics of this window is summarized below for selected energies:

E (keV)	$e^{-\mu x}$ ($x = 0.005''$)
12	0.99
10	0.98
8	0.95
6	0.89
4	0.73
3	0.46
2	0.09

It is clear that the window cuts off very rapidly below 4keV defining approximately the low-energy limit of the spectrometer.

Combining the effect of the absorption in the Be window with the energy conversion efficiency of the scintillator yields a curve which is useful in determining the required diffraction crystal. This curve, indicating the relative number of visible photons produced per incident x-ray of energy E , is shown in Fig. (2). The overall response displays a maximum near 6keV with a useful energy range from roughly 3 to 12keV. This range is consistent with first order diffraction from the 200 planes of LiF where 4.22keV x-rays are diffracted at 45° and 12.4keV x-rays at 15° . Although the range could be expanded somewhat, the experimental difficulties in looking at nearly perfect reflection (~ 3.1 keV) or grazing incidence (>25 keV) do not warrant the increase. Other crystals could be employed but would also require a redesign of the detector and window geometries.

The wavelength resolution of the spectrometer can be estimated approximately from the values given in Birks' original paper. Given that the diffraction crystal is thin, that the detection surface is approximately 60mm from the crystal, and that the collimation slits are on the order of 1mm wide, the resolution $\Delta\lambda/\lambda$ should range from about 1% at 4keV to about 3.5% at 12keV. With a flat, rather than a curved detector plane, the resolution is somewhat

degraded by the finite thickness of the scintillator and by a somewhat different dispersion along the plane.

Physical Structure

From the above considerations the spectrometer was designed and constructed. A description of the device is presented in the following. (See Fig. (3)).

The spectrometer is housed in a brass vacuum enclosure which is evacuated through the connection to the x-ray source. Evacuation is required in order to eliminate the excessive absorption of low energy x-rays in air. This connection also serves as the optical path for the x-rays from the source. A 5 mil thick pinhole-free beryllium sheet (not shown) is placed in this optical path in order to prevent the passage of visible light into the spectrometer. This sheet also serves to prevent contaminants from the source from entering the spectrometer and subsequently plating out on the diffraction crystal. The beryllium window is better than 73% transmitting for x-rays with energies greater than 4keV.

Collimation of the x-ray beam is accomplished with a two-slit system constructed from lead. Each of the 1.5mm slits are 0.5cm thick and 2.54cm wide. The two slits are spaced 5.18cm apart. Utilizing the exploding wire x-ray source to be described later in which the diffraction crystal is approximately 14.5cm from the wire, the collimation system constrains the crystal to view an x-ray source which is approximately 0.7cm in length.

The LiF analyzing crystal was manufactured by Harshaw Chemical Company of Solon, Ohio. It is 0.51cm in width and length, 1mm thick, and is bent on a radius of 0.41cm. An adjustable brass holder locates the crystal at the center of the output slit of the collimator. The 200 diffracting planes of the crystal are parallel to the cylindrical surface so as to diffract x-rays of energies in

11

the range of 4.22keV to 12.4keV in the primary order.

After diffraction, the x-rays propagate approximately 55mm to a 30 mil thick plastic scintillator sheet where they are absorbed and converted to visible photons. The NE102 scintillator is manufactured by Nuclear Enterprises, Inc. of San Carlos, California. It has an emission maximum at 423nm with the energy conversion efficiency being approximately 3 times greater for 4.22keV x-rays than for those at 12.4keV. The scintillator sheet forms a vacuum window across an 8cmx0.5cm slit on the flange at the output of the spectrometer with the seal between the window and the flange being accomplished with "Torr-Seal" low vapor pressure epoxy. In the present mode of operation the scintillations from the window are viewed by an electronic smear camera which yields a photograph of the emission spectra along the direction of the slit with the time evolution being provided in the orthogonal direction along the film. The output flange was made removable so as to provide a means for developing different detection geometries.

Exploding Wire X-Ray Source

During the contract period an exploding wire device was designed and constructed to serve as a flash x-ray source for the x-ray spectrometer. The final design, shown in Fig. (4), consists of a chamber which has been fitted to the high voltage terminal structure previously used in our plasma focus apparatus. This structure provides both the anode and cathode connections as well as the rear vacuum seal. By employing this existing unit, a considerable amount of design time was saved. The overall device is described in detail in the following paragraphs.

The chamber is basically a cylinder 13.5cm in length and 7.5cm in diameter. A wire support 2.54cm in diameter and of variable length is located along the axis of the chamber. In the present configuration this support is 10 cm in length with the last 3cm being composed of OFHC copper serving as an anode. This section is also segmented so as to provide a clamp for the wire. The two segments are held together by set screws which are not shown in Fig. 4. The wire to be exploded extends from the anode along the axis to a clamp on the flange at the end of the chamber. This flange serves as the cathode of the device. The clamping arrangement insures that the wire is taut and is exactly on axis. A second flange provides the vacuum seal at the cathode end of the chamber with the region between the two flanges being evacuated by means of holes in the wire clamp. Typically the wire is made of 10 mil tungsten and is 3.5cm in length.

The chamber is evacuated by means of a four inch oil diffusion pump topped with a refrigerated baffle. Ultimate base pressure attained by this system is 1×10^{-7} Torr although the background pressures are typically on the order of 1×10^{-5} Torr during experimental conditions. Approximately 10 minutes are required to replace the wire in the chamber and to pump this system down to this order of pressure.

As noted above, the electrical connections are made on the concentric anode and cathode terminals at the rear of the chamber. A newly designed header (not shown) provides a low inductance transition between these terminals and eight parallel six foot lengths of RG-8 coaxial cable. These cables are connected via a triggered air-gap to a capacitor bank composed of four 15 μ F low inductance condensers. The bank can be charged to a maximum of 20kV with a resultant stored energy of 12kJ. From the observed current waveform during a discharge at an ambient background pressure of 4 Torr (a condition in which the wire does

not explode) the total measured series inductance of the system is ~ 110 nh. The corresponding quarter period ring time (i.e., the time required to reach current maximum) is approximately $4\mu\text{sec}$. This time is slightly greater during an explosion event due to the increased effective radius of the wire.

A vacuum port is provided on the chamber wall for a connection to the x-ray spectrometer. This port not only serves to evacuate the spectrometer but to also provide a direct path between the x-ray source and the spectrometer collimation system. Depending upon the length of the copper anode, the spectrometer can be made to view the x-ray emission from the wire or the thick target Bremsstrahlung from the anode.

References

1. L. S. Birks, Rev. Sci. Instrum., 41 No. 8, 1129, (1970).
2. Exploding Wires, edited by W. G. Chace and H. K. Moore, (Plenum, New York), Vol. 4, p. 161 (1968).
3. S. K. Handel, B. Stenerhag, and I. Holmstiöm, Nature, 209, 1227 (1966).
4. M. J. Bernstein, Rev. Sci. Instrum., 43, No. 9, 1323, (1972).
5. Plasma Diagnostic Techniques, edited by R. H. Huddleston and S. L. Leonard, (Academic Press, New York), p. 584, (1965).

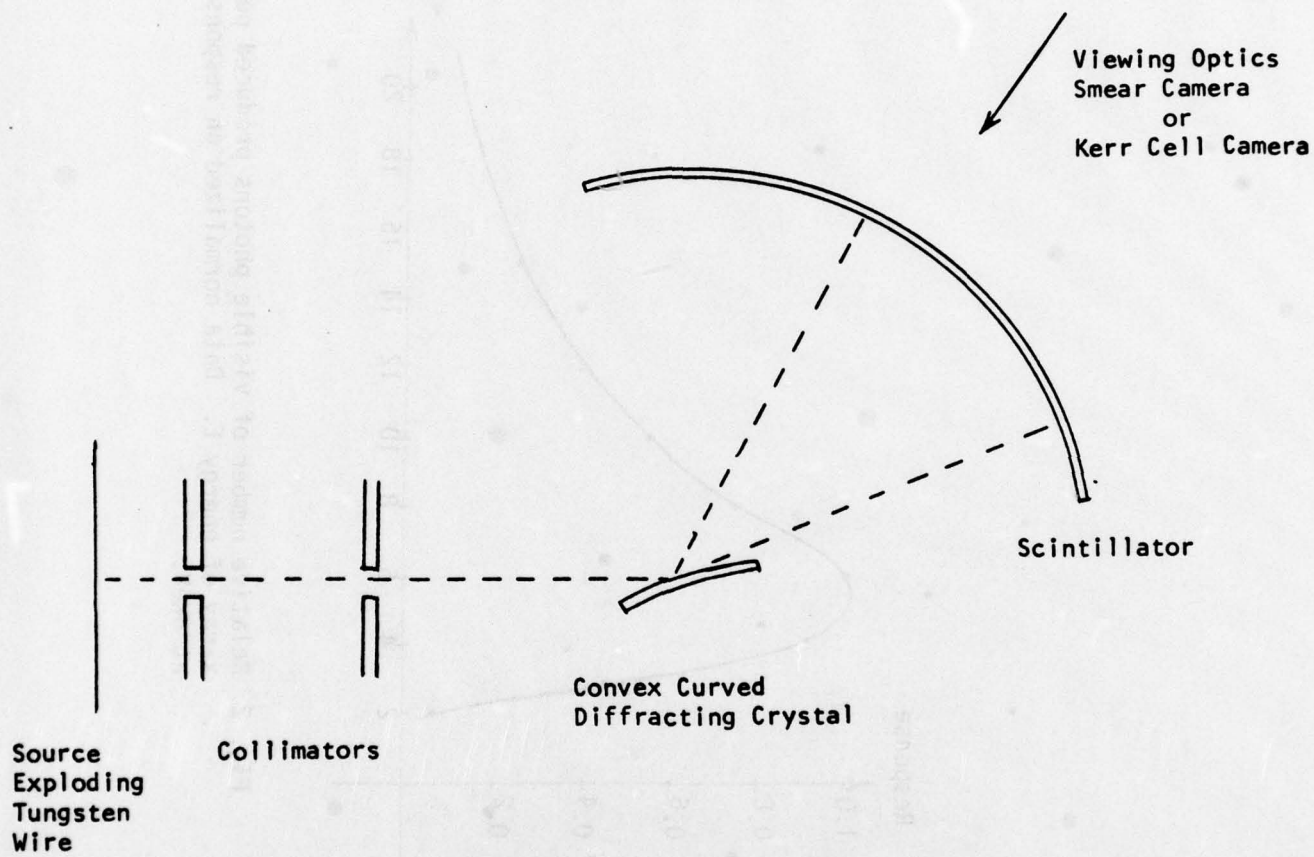


Figure 1.

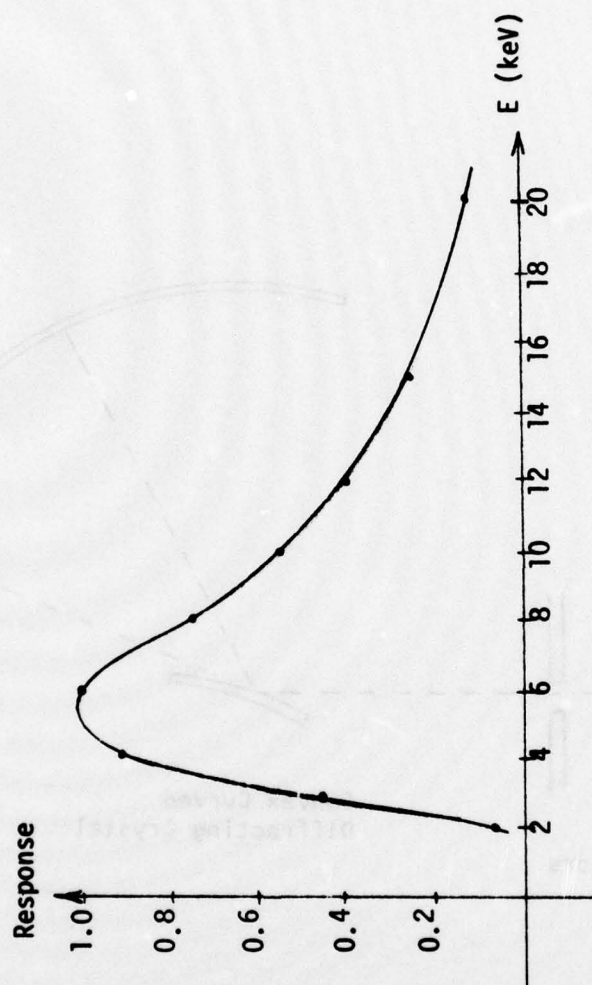


Fig. 2 Relative number of visible photons produced per x-ray of energy E . Data normalized on response at 6KeV.

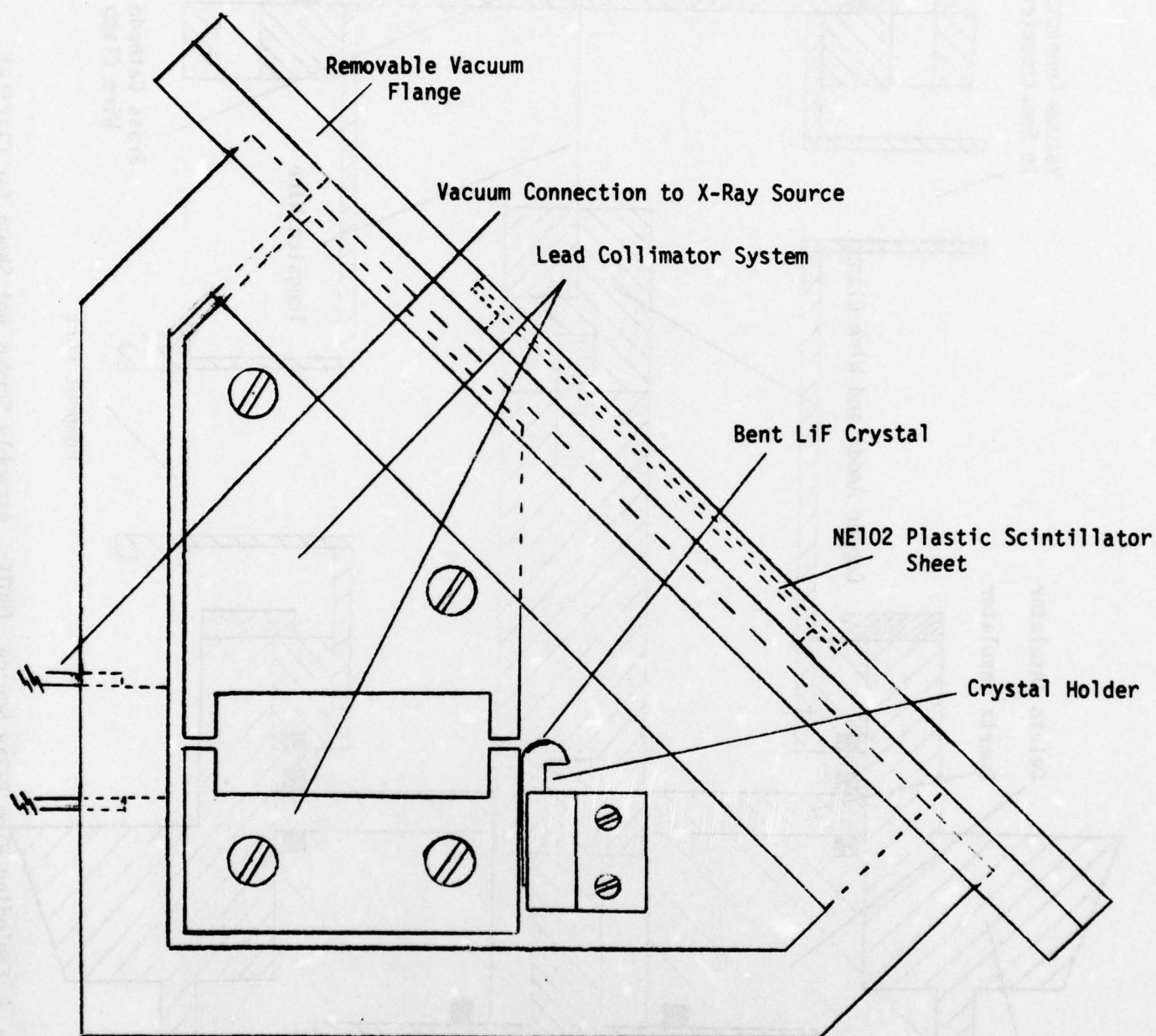


Figure 3 Convex Curved Crystal X-Ray Spectrometer
(Note: Top Plate, O-Ring Seals, and Assembly screws not shown for clarity).

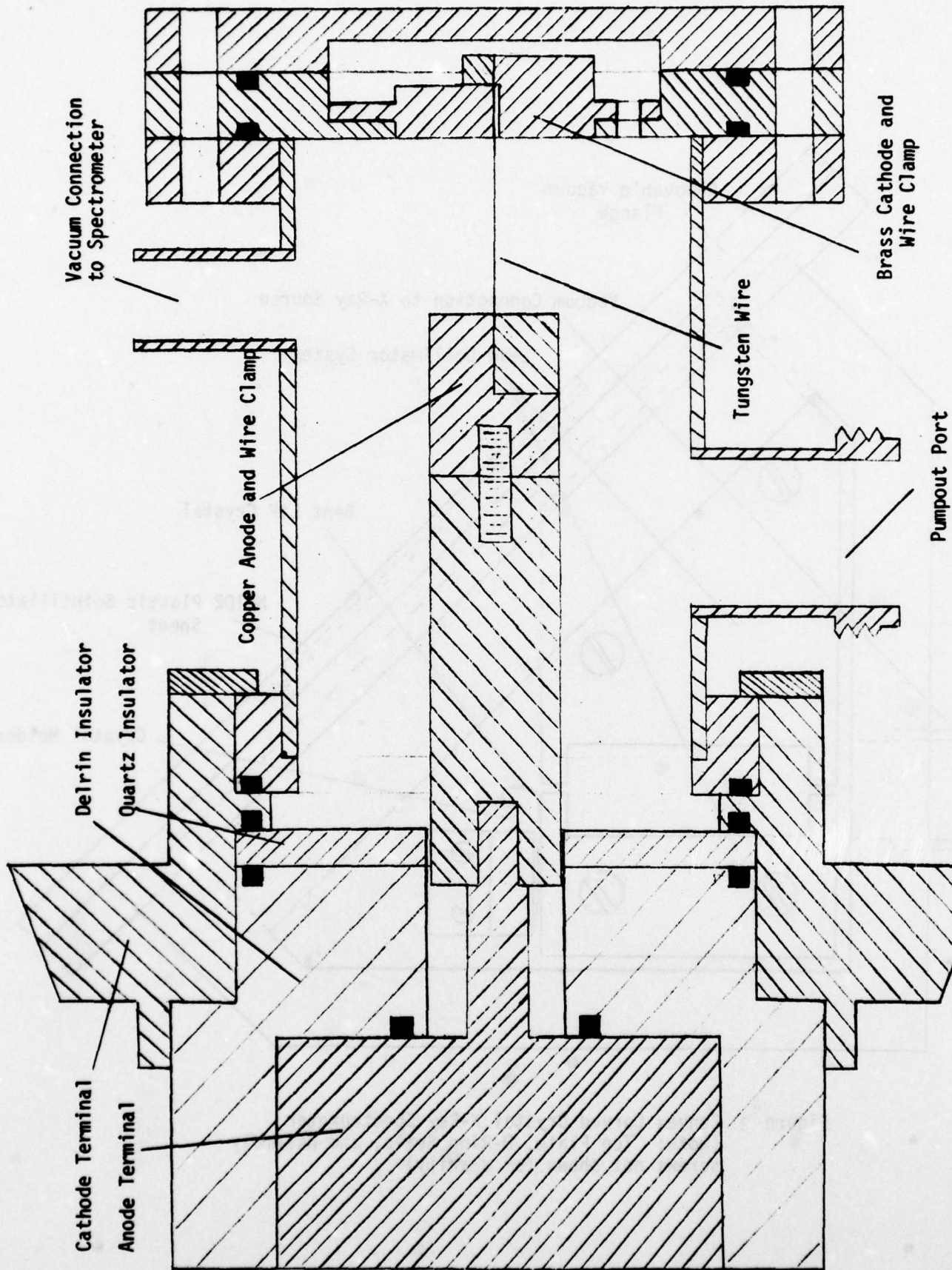


Figure 4 Exploding Wire X-Ray Source (NOTE: Assembly Screws not Shown for Clarity).

PART II

A PRELIMINARY DESIGN OF A NANOSECOND RESOLUTION X-RAY DETECTOR FOR AN X-RAY SPECTROMETER

by

RICHARD W. VESEL

CHAPTER 1

INTRODUCTION

1.1 A Basic X-Ray Spectrometer System

The presence of intense flash x-ray sources in the laboratory has increased greatly in the recent past. Continued research into the characteristics of the dense plasma focus and laser generated plasmas, as well as a renewed interest in exploding wires and foils, has pointed out the need for a suitable X-ray spectrometer capable of yielding time-resolved information on individual events. The duration of these events is quite short, that is, anywhere from 1 to 1000 nanoseconds. Observation of time resolved X-ray spectra is a requirement in order to develop a clear understanding of the X-ray generation mechanism.

A search of the available literature reveals that no such device exists at present. Detailed X-ray spectra, even on a time average basis, have not been able to be measured in single event short duration plasmas.

Currently, there is no method available to the researcher to obtain time resolved continuous spectra. Existing equipment uses Ross filter pairs coupled with silicon diode detectors⁽¹⁾ or scintillator/foil band-pass filters with photomultiplier detection.^(2,3) These filter techniques are capable of providing time resolution down to a few nanoseconds. However, they are only useful for detecting small energy ranges. Thus, to achieve any degree of spectral resolution, a large number of these units and the associated recording devices are required. This sacrifices any sort of spatial resolution and, needless to say, much money.

Other methods are available for obtaining continuous spectra from a source. They are the focusing crystal⁽⁴⁾ and the convex curved crystal, the latter method based on Bragg diffraction and developed primarily by L. S. Birks.⁽⁵⁾

As originally described, these methods required the use of photographic emulsions whose sensitivity is quite low. The spectra thus obtained could be of extremely high resolution, but were obviously not time resolvable. Many events were required to produce enough X-ray flux to provide sufficient film darkening in these experiments. However, Birks stated that if the emulsion in his device were replaced by a scintillator and suitable optical detector, time resolution could be obtained. (See Fig. 1).

If one were to use a series of photomultipliers in viewing the output scintillator of such a device, its advantages would be lost for the same reasons which make the filter techniques impractical. In fact, such a device would be even more impractical due to the low diffraction efficiency of the curved crystal.

What is required with a Birks type spectrometer is a detector which must be continuously distributed over the output plane of the spectrometer, have the required time resolvability and sensitivity, and it must have an output which can be read conveniently.

The wide range of photoelectronic imaging devices currently available are capable of providing this type of detector.

21

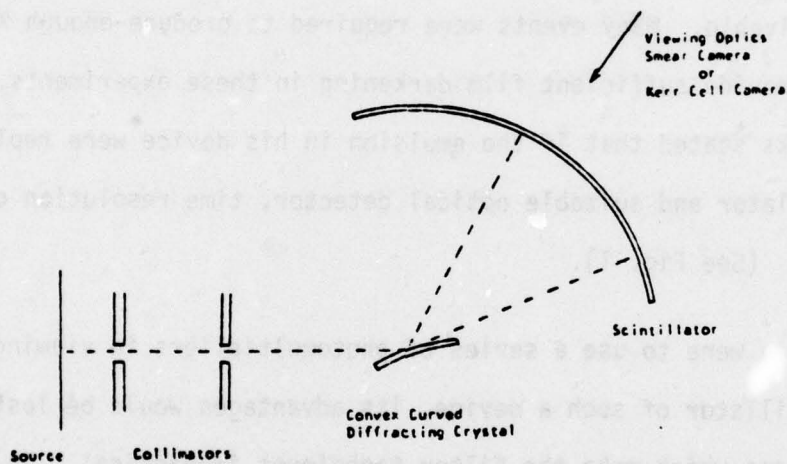


Figure 1.

A Birks-Type Spectrometer With
Scintillator Output Window

X-ray image converters have been developed for use in X-ray spectrometers,⁽⁶⁾ industrial applications,⁽⁷⁾ and for medical diagnostics.^(8,9) High sensitivity is the only prerequisite for these cases as no time resolvability is required. However, Bernstein and Hai developed a time resolved X-ray pinhole camera using a beryllium shielded scintillator and an image converter camera,⁽¹⁰⁾ but it did not have the sensitivity required in our present application.

These ideas are to be combined, then, to achieve a time resolvable X-ray spectrometer. A Birks type convex curved crystal spectrometer will diffract X-rays onto a plastic scintillator. This scintillator is to be observed by a high-sensitivity (large gain) gatable imaging device. The output of this device must be a signal which is capable of providing recordable quantitative data.

At the onset of the project, it was proposed that a commercially available intensified vidicon tube was capable of meeting these requirements⁽¹¹⁾ since a) it had the sensitivity and b) the output would be in a convenient video-type format. It also had the added attraction of being capable of storing the image of the scintillator for long periods of time.

1.2 Purpose of the Thesis

It is now the purpose of this thesis to describe in detail how the imaging device was chosen and what the details of the supportive circuitry are. This will involve first a description of two X-ray sources, the exploding wire and the electron gun. Their outputs were

characterized so that quantitative determinations could be made with which to specify the imaging device. Secondly, the spectrometer, which was constructed previous to the author's involvement with the project, will be characterized to give more information as to the requirements of the imaging device.

Lastly, the entire detection system which includes the use of a storage device (a video disk system) will be described. This should enable the reader to see how the concept of the time-resolvable X-ray spectrometer was taken from the block diagram stage (see Fig. 2) to the hardware device itself.

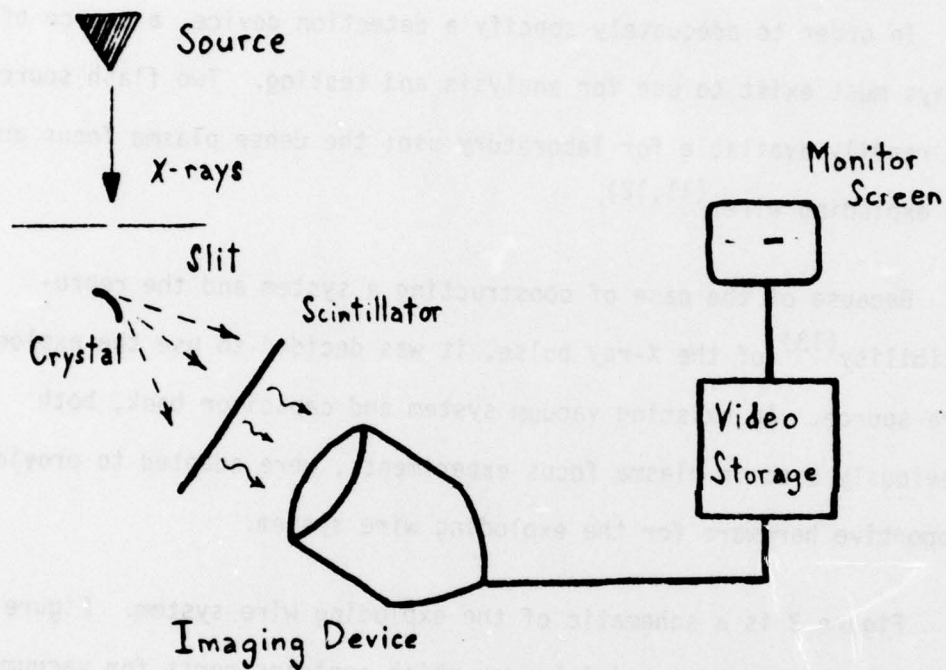


Figure 2.

Schematic of the Time Resolvable X-Ray Spectrometer

CHAPTER II

THE X-RAY SOURCES

2.1 The Exploding Wire

In order to adequately specify a detection device, a source of X-rays must exist to use for analysis and testing. Two flash sources are readily available for laboratory use; the dense plasma focus and the exploding wire.^(11,12)

Because of the ease of constructing a system and the reproducibility⁽¹³⁾ of the X-ray pulse, it was decided to use the exploding wire source. An existing vacuum system and capacitor bank, both previously used in plasma focus experiments, were adapted to provide supportive hardware for the exploding wire system.

Figure 3 is a schematic of the exploding wire system. Figure 4 is a drawing of the coaxial header which contains ports for vacuum and diagnostic connections as well as electrical connections.

The vacuum system is capable of pumping to pressure of less than 10^{-7} torr, but the explosions were usually done with background pressures of between 10^{-6} and 10^{-5} torr. The capacitor bank voltages were varied from 10 to 15 kilovolts before they were discharged through the wire.

The total capacitance of the system is $60\mu\text{f}$ in the form of four parallel $15\mu\text{f}$ low inductance high voltage capacitors. This bank is capable of storing up to 12 kilojoules. The inductance of the system

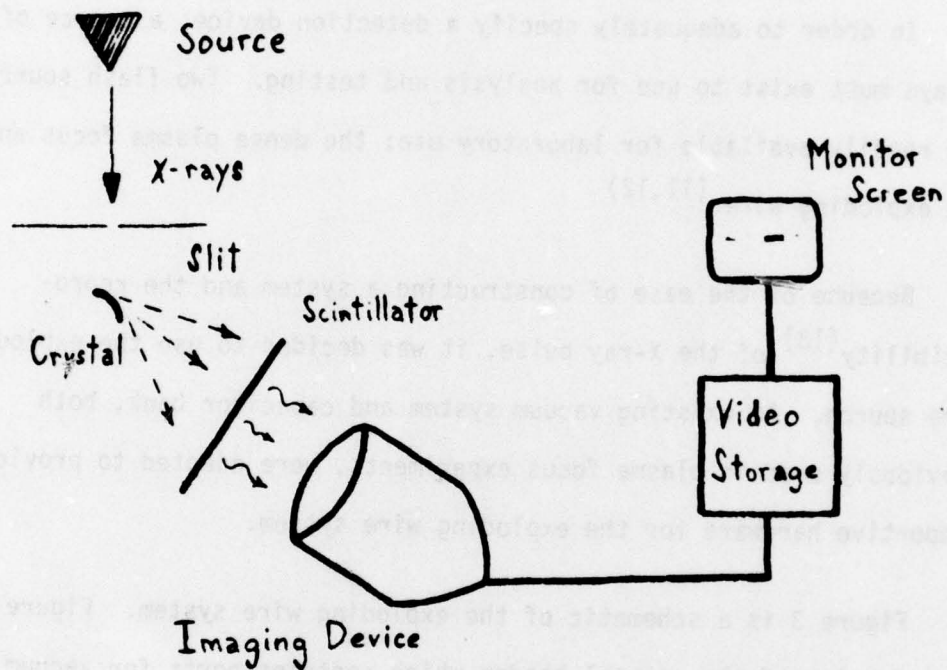


Figure 2.

Schematic of the Time Resolvable X-Ray Spectrometer

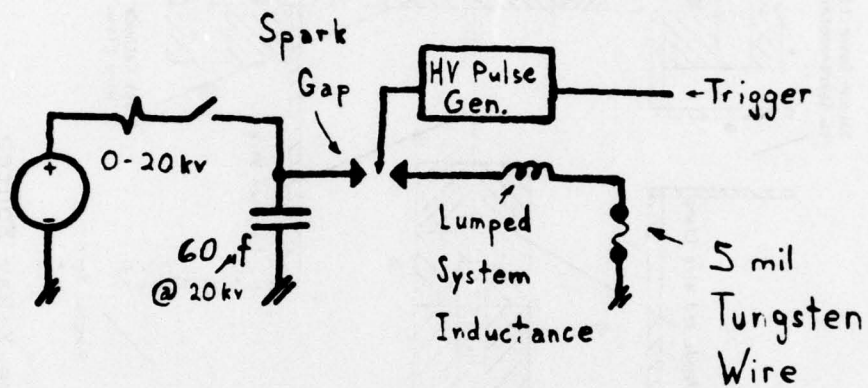


Figure 3.
Electrical Schematic of the Exploding
Wire System

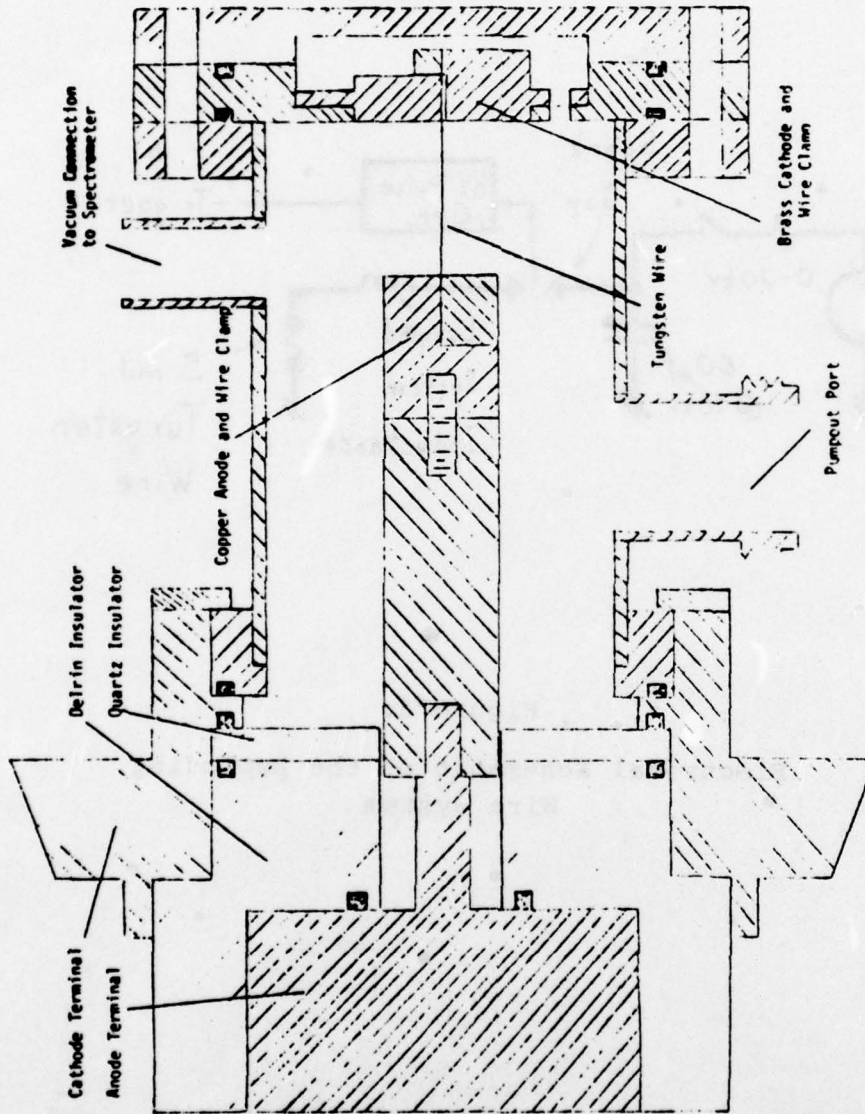


Figure 4. Exploding Wire X-Ray Source

is distributed in the wire, its support, the coaxial header, and in the 8 parallel six foot lengths of RG-8 cable connecting the capacitor bank to the coaxial header.

The calculated value of the total inductance is approximately 160 nanohenries. Thus, a calculated LC constant yields a prediction of a $4.9\mu\text{sec}$ quarter period ring time as the capacitor discharges and the LC circuit rings.

In order to provide a check of these values and to look for the current breaks⁽¹⁴⁾ observed by others in the discharge, a Rogovski coil was mounted around the inner conductors of one of the RG-8 cables. Figure 5 is an oscillograph of the dI/dt signal during a typical discharge. Note the current breaks during the initial stages of the discharge. Also note that the quarter period ring time is approximately $4\mu\text{sec}$. Thus, the system has an observed inductance of approximately 110 nanohenries, depending upon the tolerances of the capacitor values.

2.2 Characterization of the X-Ray Pulse

Two characteristics of the X-ray output from the exploding wire had to be obtained. First, a time scale observation had to be made to see if the results agreed with previous experiments.⁽¹⁵⁾ Secondly, the intensity of the pulse had to be estimated and then measured in some manner. In the latter area, there has been no published data, leaving only the original proposed estimate of a source strength of approximately 10^6 ergs/sr.⁽¹⁶⁾

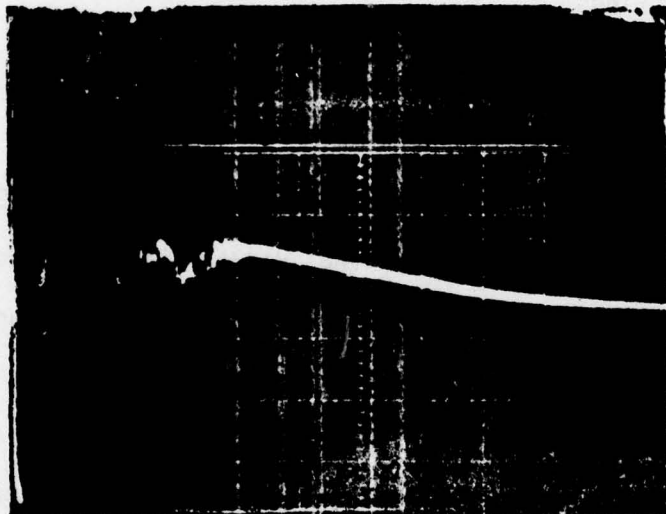


Figure 5.

dI/dt for an Exploding Wire Event

(NOTE: Horizontal scale is
1 $\mu\text{sec}/\text{div.}$ and trace
starts one division
in from edge.)

In order to obtain a time scale observation, the X-rays had to be converted to a recordable electrical signal. This was achieved using a scintillator-photomultiplier combination at the diagnostic port. Two 30 mil by 1.6" scintillator⁽¹⁷⁾ disks were placed in front of a beryllium (.002" pinhole free)- scintillator vacuum window on the output port. A light-tight aluminum foil tube surrounded the scintillator disks and one end of the tube was placed around the vacuum window. The other end led to the faceplate of a photomultiplier tube (PMT) biased at 1800 volts.

As a wire was exploded, X-rays (but no visible light) passed through the beryllium and hit the scintillators. Their glow registered on the PMT. After amplification of this signal, it was traced out on an oscilloscope and recorded photographically. Figure 6 shows a schematic of the technique used.

Previous work with a system of relatively the same inductance but lower capacitance (.4 μ f versus 60 μ f)^(15,18) yielded X-ray output pulses which had from 20 to 30 nanosecond half widths. Figures 7 and 8 show results from our exploding wire source. Both photographs in Figure 7 show half-widths of approximately 300-400 nanoseconds while Figure 8 shows it to be about 500 nanoseconds. Note that the pulses are roughly the same shape as those obtained by Handel et al.,^(12,18) and that in Figure 8, a restrike output was also obtained several hundred nanoseconds after the initial pulse was extinguished. This is a phenomenon which was also observed by Handel and co-workers.⁽¹⁹⁾

31

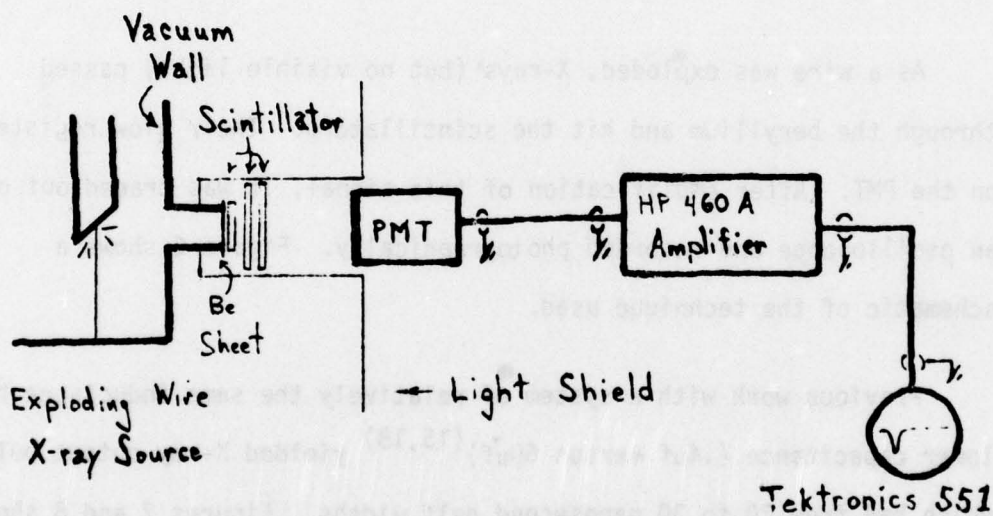
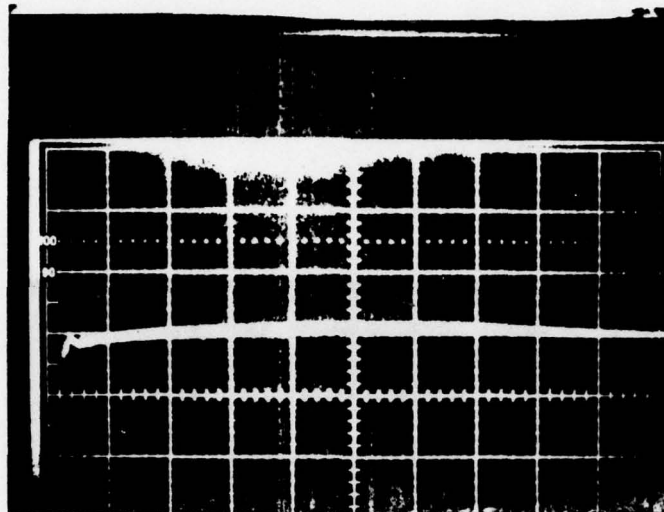


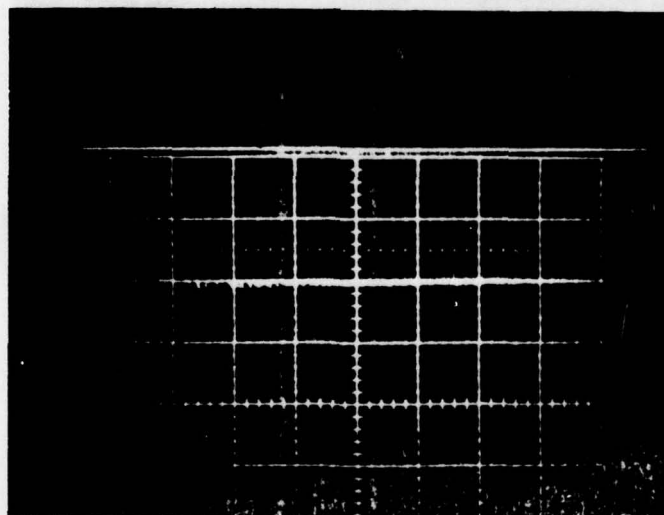
Figure 6.

Schematic of Time Scale Experiment

THIS PAGE IS BEST QUALITY PRACTICABLE
FROM COPY FURNISHED TO DDG



a)



b)

Figure 7.

PMT Signal for Two Explosions

a) Hor. Scale; 2 μ sec/div.b) Hor. Scale; .5 μ sec/div.

& trace starts 1 div. in

THIS PAGE IS BEST QUALITY PRACTICABLE
FROM COPY FURNISHED TO DDG

15

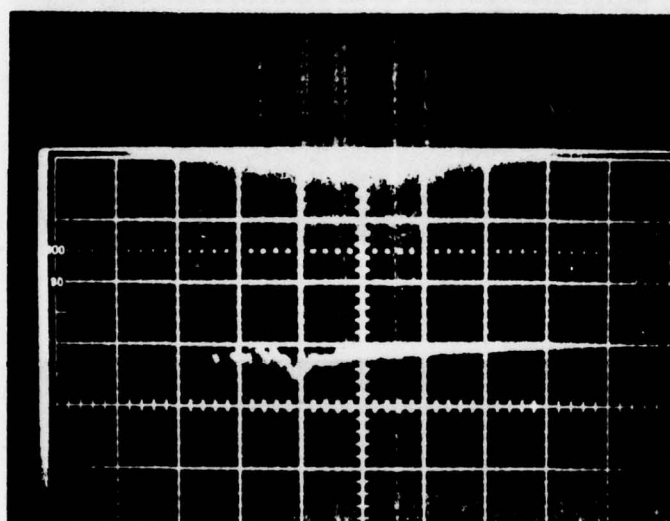


Figure 8.

An X-Ray Pulse With Restrike

(Hor. Scale is $.5 \mu\text{sec}/\text{div.}$
& trace begins one division
in from edge.)

These results, therefore, show that we may expect an X-ray pulse from a wire exploded in this system to last in the vicinity of 500 nanoseconds. This is long enough to yield several 10 to 100 nanosecond spectral frames within the duration of such events.

Obviously, the next step is to try and obtain an estimate (based on experiment) of the intensity of such X-ray pulses. The route chosen to do this was to compare this source strength to that of some known, or calibratable source. This required the construction of a calibratable source, namely, an electron gun.

The electron gun was constructed and mounted in a brass plate in place of the brass cathode and wire clamp shown in Figure 4. Figure 9 shows the electrical schematic of the electron gun with the high voltage accelerating supply attached to the anode. Another modification was made to the anode inside the vacuum chamber. The flat copper anode was replaced by a copper anode with a 45° slant on its face directed toward the diagnostic port. This was done to increase the X-ray flux directed at the port for both the e-gun, and the exploding wire.

Figure 10 shows the electron gun mounted in place on the vacuum system and chamber. The high voltage supply attached directly to the gun is capable of striking an emission from the gun with approximately 2 kV of accelerating potential. Additional energy is imparted to the electrons by the high voltage supply biasing the anode. It is capable of giving the beam a final energy of ~ 30 kV.

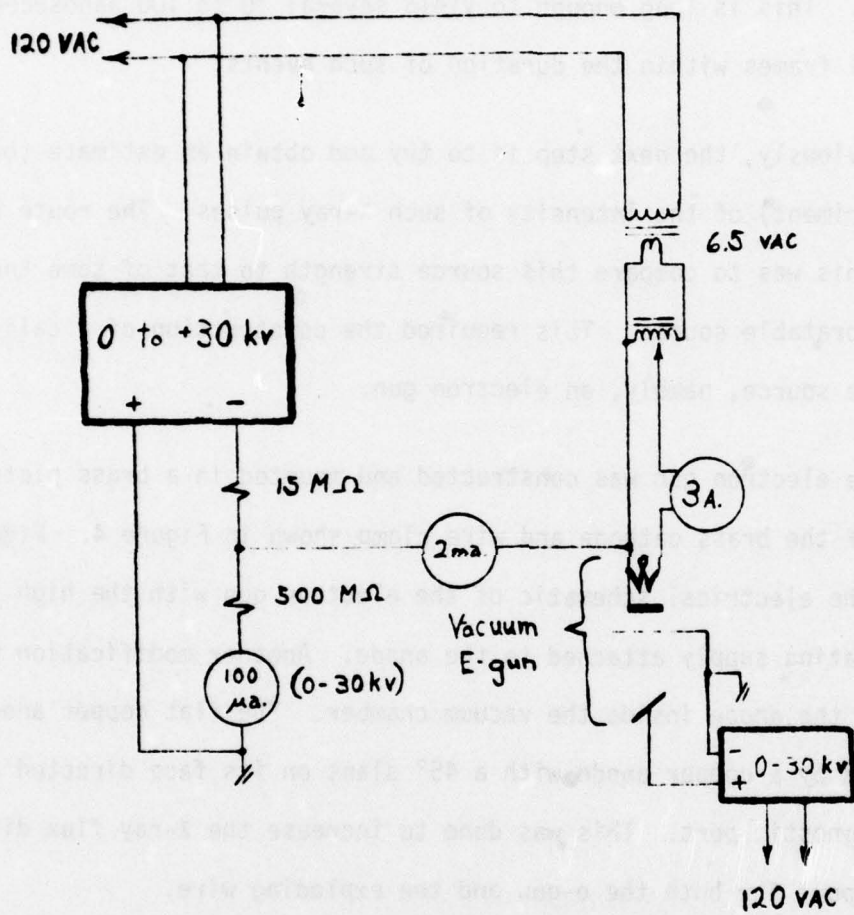


Figure 9.

Schematic of Electron Gun System

THIS PAGE IS BEST QUALITY PRACTICABLE
FROM COPY FURNISHED TO DDG

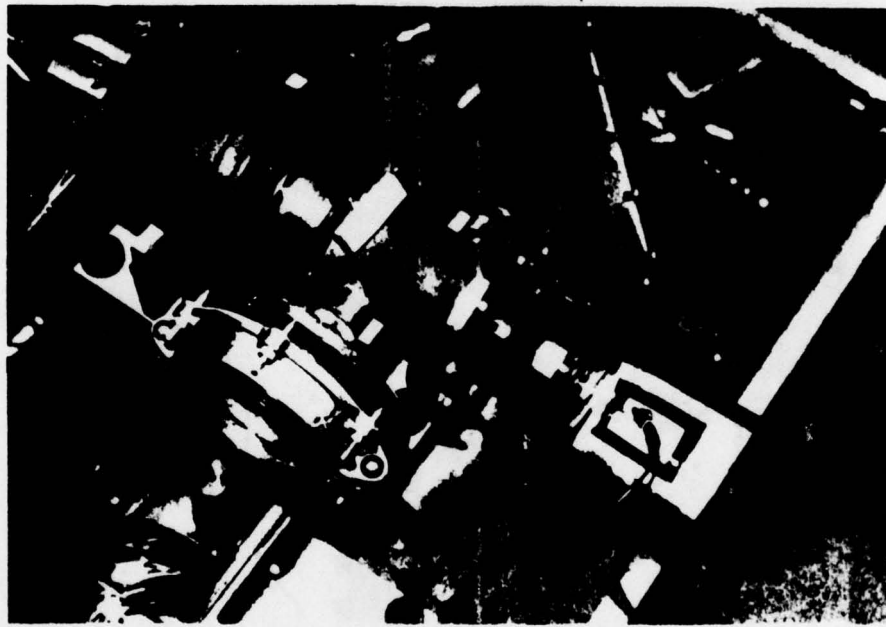


Figure 10a.

Electron Gun (Lower right) on Vacuum
Chamber

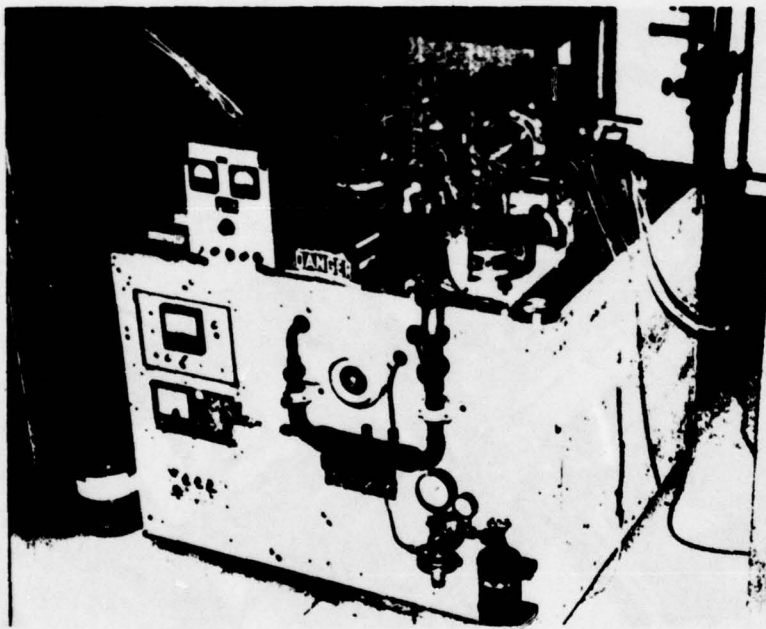


Figure 10b.

Vacuum System and High Voltage Electron
Gun Supplies

Calibration was done by means of calculation and comparison of film darkening. X-rays are generated at the anode surface by thick target bremsstrahlung using the e-gun. We also modeled the exploding wire as generating X-rays in the same manner to obtain an order of magnitude estimate of its strength.

With a current i impinging on a thick target after being accelerated by a voltage V , the resulting X-ray flux has intensity I_t given by the formula, (20)

$$I_t = i a_1 Z V^2$$

for copper, $a_1 = 1.2 \times 10^{-9}$ and $Z = 29$. The total energy is then given by

$$E = I_t \cdot t$$

where t is the duration of the event. If i is a function of time, then so is I_t which would then require an integral expression to find E rather than a simple product. However, in order to achieve a simple estimate of the X-ray flux, i will be held constant at some average value for the duration of the event.

A plate of Polaroid Type 57 film was placed in front of the beryllium-scintillator vacuum window while still in its light-tight packet. After exposing the film to an X-ray burst from the exploding wire, the film was developed. The same procedure was followed with the electron gun. Film was exposed to X-rays produced by the e-gun for periods lasting from several seconds to 5 minutes. These exposures

were then matched visually with the various pictures from the exploding wires. Matching was done by comparison of gray color (degree of exposure) and those closest to one another were then paired.

The table below gives a typical mid-range result for one such experiment.

Table 1. Intensity Calculation for X-ray Source Strength

	<u>Exploding Wire</u>	<u>E-Gun</u>
Voltage (V)	14.6 KV	11 KV
Current (i)	~ 10 k maps (12,14,18)	.21 ma
Time (t)	300 nsec	30 sec
Intensity (I_t)	7.4×10^4 watts	8.8×10^{-4} watts
Energy ($I_t \cdot t$)	2.2×10^{-2} joules or 2.2×10^5 ergs	2.6×10^{-2} joules or 2.6×10^5 ergs

These values for E correspond to approximately 2×10^4 ergs/sr as a source strength, not nearly as high as estimated in the original proposal.⁽¹⁶⁾ However, the results as shown in Table 1 are in agreement with the visual matching. Thus, they have been accepted and will be used later in calculating the spectrometer efficiency and required detector sensitivity.

CHAPTER III

THE CURVED CRYSTAL SPECTROMETER

3.1 Characteristics of the Spectrometer

Design and construction of the curved crystal spectrometer was carried out previous to the author's involvement with the project. Its form follows that described by Birks⁽⁵⁾ with a few minor changes. As shown in Figure 11, two collimators were used to develop a 2mmx4mm spot on a bent LiF crystal. The cylindrical section, which the crystal was shaped to, made the 4mm spot length correspond to the z direction and the 2mm width to the azimuthal direction (cylindrical coordinates).

A .001" beryllium window was added to each collimator along with glass wool packing in the non-critical paths to eliminate light leakage into the spectrometer. The scintillator output window was made flat rather than curved (as was described in Figure 1) in order to facilitate easy optical focusing of the output scintillator window (hereafter referred to as "the window").

Simple first order Bragg diffraction by the crystal was intended to yield an output 5 cm wide across the window, representing a useful range of from 4 to 14 keV photon energy. The window material chosen was NE 102 plastic scintillator in sheet form, .9mm thick. This thickness was calculated to give the best balance between absorption of the X-ray photons, which would go down as thickness decreased, and resolution

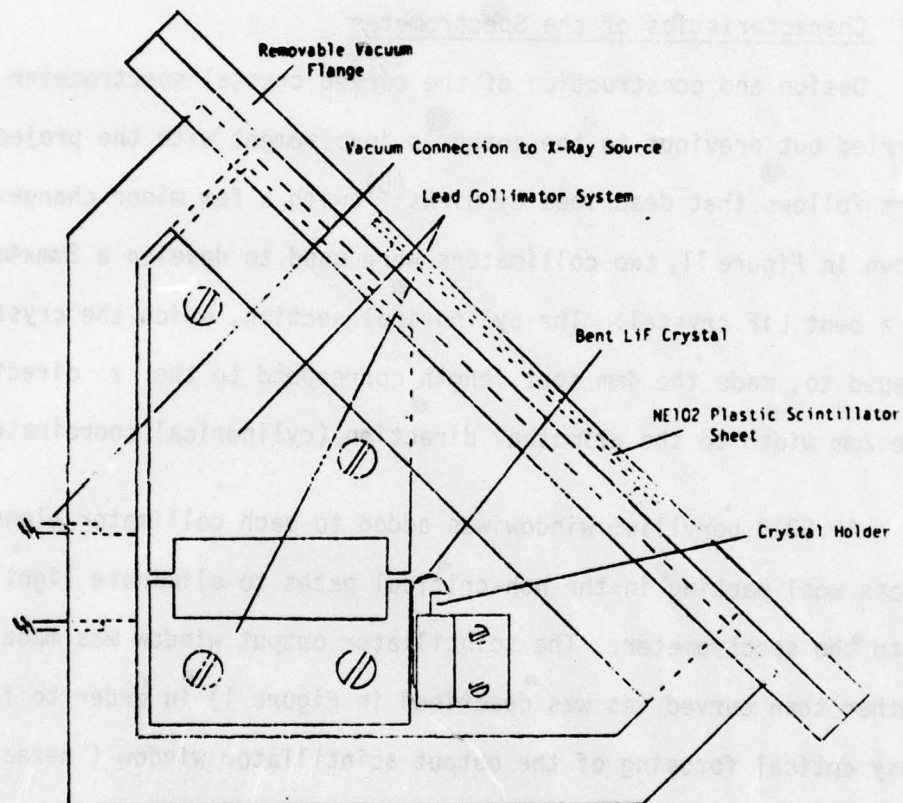


Figure 11.

Convex Curved Crystal X-Ray Spectrometer

(NOTE: Top Plate, O-ring Seals,
Assembly Screws, Beam Trap,
Glass Packing and Beryllium
Windows not Shown for
Clarity.)

which would get worse as thickness increased. The scintillator had a several thousand angstrom layer of aluminum vacuum deposited on the inside which would essentially double the efficiency of the output in the direction of the detector.⁽²¹⁾ This choice of scintillator also yielded a reasonably constant absolute quantum efficiency from the range of 1-10 keV. ^(21,22) Personal communications with Nuclear Enterprises stated that this quantum efficiency is about 2.5%, which is much better than the generally accepted figure of .6% for most plastic scintillators. Last of all, NE 102 has a decay time of 2.4nsec, which makes it fast enough for the time resolution stated in the design goals.

Spatial resolution is stated to be aperature limited. Other contributing factors to resolution degradation are the thickness of the scintillator and the crystal thickness.⁽⁵⁾

3.2 Sensitivity of the Spectrometer

Sensitivity will be defined here as the output which one can reasonably expect to see at the window when a certain flux of X-rays enters the spectrometer. The value to be examined is the output flux, F_1 , in watts/m² at the window.

$$F_1 = I_t \cdot \gamma \cdot e_1 \cdot e_2 / A \quad , \text{ where}$$

I_t = Intensity of the source (watts)

γ = (Flux incident on crystal/total flux)

e_1 = Diffraction efficiency of the crystal = (No. diff/No.incident)

e_2 = Conversion efficiency of NE 102 scintillator in window

$$= \alpha \cdot \text{absorption} = \alpha \cdot A_b$$

α = Absolute quantum efficiency (2.5%)

A_b = Absorption in NE 102 = $1 - e^{-\mu x}$

$$\mu = \frac{2.37 \cdot 10^3}{E^3}, \text{ where } E = \text{photon energy in keV}$$

x = Thickness of Ne 102 in cm (.091 cm)

A = Area of NE 102 exposed to diffracted beam (m^2)

We shall calculate these various constants here.

For $E = 10 \text{ keV}$ $A_b = .19$

$$\text{Thus } \underline{e_2 = 4.8 \times 10^{-3}}$$

Birks⁽⁵⁾ has stated that e_1 is essentially 1 in 1000.

$$\underline{e_1 = .001}$$

To find γ we must find what distance the crystal sits from the source. Direct measurement sets this value at 150 mm. Therefore, assuming isotropic radiation of the source and assuming the source is a point source,

$$\gamma = \frac{\text{spot size}}{4\pi r^2} \quad r = 150 \text{ mm}$$

$$\text{spot size} = 8 \text{ mm}^2$$

Thus,

$$\gamma = 2.8 \times 10^{-5}$$

Note that this is the worst case for γ . If radiation is radiated preferentially away from the anode face or if the crystal is placed closer to the source, γ may be substantially improved. Also, the source is not a point source, a fact noted by several investigators, (11,13,14) which would also tend to increase γ .

Using $I_t = 7.4 \times 10^4$ watts for the case of an exploding wire as a source, we obtain (for $A = 2 \times 10^{-4} \text{ m}^2$)

$$F_1 = 5.0 \times 10^{-2} \text{ watts/m}^2$$

Photoelectronic imaging devices usually specify sensitivities with respect to foot-candles at the faceplate of the device. Thus, F_2 will be expressed in these units

$$F_2 = F_1 / .0173 = 2.9 \text{ H ft. candles}$$

This figure is, of course, a general luminosity figure. Appendix 1 contains a graph of the relative response of the output window across its useful output range.

3.3 Tests Performed on Spectrometer

Noting that the value of A_b is 19%, the remainder of X-rays incident on the window pass through. These may be detected by photographic plates to observe if actual spectra are being generated by the spectrometer. To obtain exposure levels equivalent to those achieved by placing film directly in front of the diagnostic port, long exposure times are required. An exposure multiplication factor, ρ may be

estimated by the expression

$$\rho = \frac{1}{e_1} \cdot \frac{\text{Area of NE 102}}{\text{Spot size}}$$

yielding $\rho \approx 2.5 \times 10^4$

This means a piece of film must be clamped over the window of the spectrometer for 25,000 wire explosions or for about 12,000 minutes of exposure to an e-gun generated X-ray source. Obviously, a more sensitive film than the Poloroid Type 57 is needed.

X-ray crystallography uses Kodak Medical X-ray type NS safety film. This film is designed for high sensitivity to X-rays. A plate of it was taped in front of the window and exposed to an $\sim 13.5 \pm .5$ kV electron beam of $110\mu\text{a}$ strength for a period of 5 hours.

It was then developed in the normal manner for this type of film. Figure 12 is the result. The heavy lines are K_α emission from the copper anode in the vicinity of 7.6 keV. Some fine structure is also visible at higher energies, while only a continuum is observable below the K_α lines.

In addition, ρ is a significant number. It is an order of magnitude estimator of the gain necessary in the photoelectric detector.

THIS PAGE IS BEST QUALITY PRACTICABLE
FROM COPY FURNISHED TO DDC

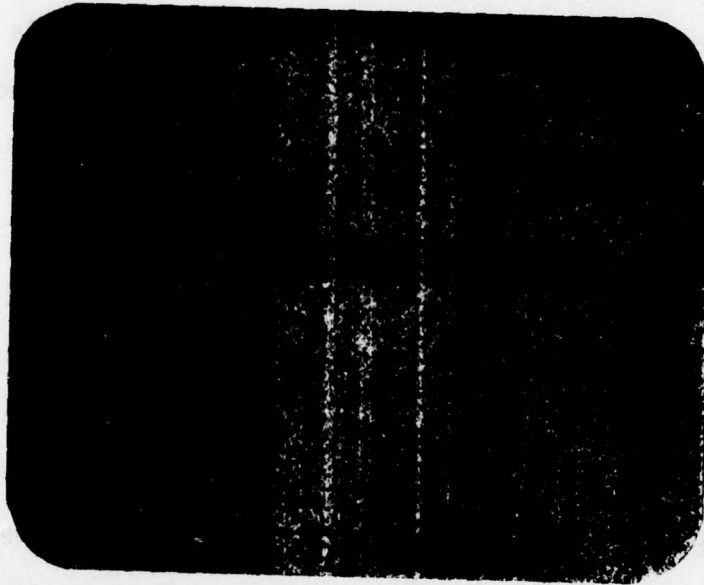


Figure 12.

Output Spectrum Obtained Using Electron Gun

CHAPTER IV

HIGH SENSITIVITY VIDICON CAMERA SYSTEM

4.1 Requirements of the Detector

The data presented in Section 3.2 and 3.3 state qualitatively that the detector must be quite sensitive. The originally proposed detector scheme involved the use of an SEC (secondary electron conduction) vidicon tube. Prior to the author's involvement with this project, a Westinghouse WL-30691 tube and specifications were obtained.⁽²³⁾ Thus, the first set of calculations deal with the suitability of this tube as a detector.⁽²⁴⁾

The SEC vidicon is a low lag device. This means that approximately 90% of the information stored on the target of the tube is read off after the first field. Therefore, one can expect reasonable signal current levels ($\geq 20\text{na}$) for $1/60$ of a second (.017 seconds). In this period of time, a resolution of 275 TV lines per raster height is possible. In order to obtain this type of performance from a WL-30691, a faceplate illumination level of approximately 4×10^{-4} ft.c. (foot candles) is required.

We will assume, for the moment, that a lens system is available which is capable of intercepting and focusing enough light from the spectrometer window to achieve the same light levels at the faceplate of an image tube as is found at the window.

We now define a time t_e which will be an exposure length for a

frame taken by the tube. (This brings in another requirement of the imaging device. It must be gatable for times on the order of t_e . This will be discussed further in this section and later on.) If t_e is taken to be 100 nanoseconds, about 10 times the proposed value,⁽¹⁶⁾ an effective illumination level at the tube faceplate may be calculated.

$$L.L._{eff} = \text{Illumination at the faceplate} \times \frac{1 \times 10^{-7} \text{ sec.}}{.017 \text{ sec.}}$$

From the data given in Section 3.2, we obtain

$$L.L._{eff} = 1.7 \cdot 10^{-5} \text{ ft.c.}$$

Clearly, a tube about 20 times more sensitive is required to have even a marginally adequate device.

After examination of several possibilities, a custom coupled package consisting of a Westinghouse WX-31381 SEC vidicon and a Varo 8605 diode intensifier was purchased. The intensifier adds a gain factor of 60 (minimum) to the performance of the SEC vidicon. In addition, the WX-31381 is a gatable tube, whereas the WL-30691 was not. At the time of purchase, Westinghouse stated that they had no experience gating this tube for $t_e < 1 \mu\text{sec.}$ ⁽²⁵⁾ It was therefore decided to go ahead and try to operate the tube in the sub-microsecond (10-100 μsec) range since no reason was given against such operation at the time.

4.2 Electronics for the Camera Head

The vacuum electron currents and high voltages used in the tube

require suitable magnetic shielding and electrical insulation. The tube was mounted in a section of 6 inch PVC cylinder with a five layer wrapping of 14 mil μ -metal around the outside. The tube is held in place in the interior of the tube by 1/4" plexiglass disks mounted between the ring electrodes. These also provided stand-off insulation between the electrodes. The rear plate for the insulation cylinder is soft steel to provide a magnetic short circuit for the μ -metal wrapping.

A case made of 1/4" aluminum plate (alloy 6061) was made to house the entire camera assembly in order to isolate the internal electronics from the 60 kc ringing frequency from the exploding wire apparatus. The skin depth of aluminum at this frequency is approximately 1 mm, so good AC shielding is provided for use in a high noise environment. The front face of the case is 1/4 steel plate, again for magnetic shielding purposes.

The various support electronics used in the camera head were either built or purchased in accordance with the specifications sent with the coupled tube package. See Appendix 2 for the specific data on the tube package. One great savings of time and effort was the acquiring of the video processing board and sweep generation board from an already existing camera design.⁽²⁶⁾ The video board is a Telemation DWG No. 01-013377-001. The sweep board is a Telemation DWG No. 01-013373-001. These boards generate the majority of the signals necessary to drive the scanning and low voltage sections of the tube along with processing the video output signal. It is recommended here that

the TMC-1100 instruction manual ⁽²⁶⁾ be used as a reference for obtaining details about circuit description and operation.

The generation of a composite video signal was chosen in order to make interfacing to existing video storage systems easy. Thus, a sync board based on National Semiconductor's MM 5320N sync generator chip was constructed from schematics available in the TMC-1100 manual. This board interfaces with the other two Telemation boards to provide a video output signal in compliance with the EIA RS-170 sync standard.

Some modifications were made to these boards in order to make them compatible with the tube package and its focus and deflection coils. These are listed and/or shown in Appendix 3. Full schematics for these portions of the camera head will be found in a forthcoming instruction manual for the camera.

In addition to the circuitry necessary for the operation of any standard black-and-white TV camera, this tube package also requires high voltage biasing and electronics to generate the gating pulses. ⁽²⁷⁾ The gating pulses are applied to the focus electrode of the intensifier section of the SEC tube. If a signal of -1.1 kV is applied to this electrode, the tube is turned off. Therefore, wanting to gate the tube on, a +1.1 kV signal is applied to this electrode in order to raise it to its normal operating potential of -7.5 kV (see Appendix 2).

In order to avoid injecting noise into the biases on the other electrodes, a separate high voltage supply, a Venus Scientific ST-10N,

51

is used to set the operating potential of the focus electrode. The camera is to be used in both a continuous and a gated mode of operation. Therefore, the ST-10N must have two input voltages, one for each operating mode. The circuit used to control the ST-10N and generate the gating pulses is shown in Figure 13.

The 2D21 is a thyatron. The plate of the thyatron is biased to a high voltage by the Venus K-30 high voltage supply. Inputs gate on the thyatron, sending a pulse down the delay line. The pulse reaches the end of the delay which is open circuited. It is reflected, returning to the plate pin on the 2D21, switching it off. The output at the cathode is then a square pulse with amplitude of +1100 volts and duration determined by the formula

$$t_e = 10\ell \text{ nsec.}$$

where ℓ is the length of the delay line in meters. Figure 14 is a photograph of the high voltage pulsing unit, while Figure 15 shows output pulses from this unit.

There are two high voltage biasing sections, one for the intensifier and imaging sections and one for the reading beam scanning section. Simple high impedance voltage dividers were used in each case along with a high voltage supply for each divider. Figure 16 shows the schematics for these biasing networks. A filter capacitor is included in the imaging network in order to remove some of the 40 khz noise from the oscillator in the -24 kV high voltage supply.

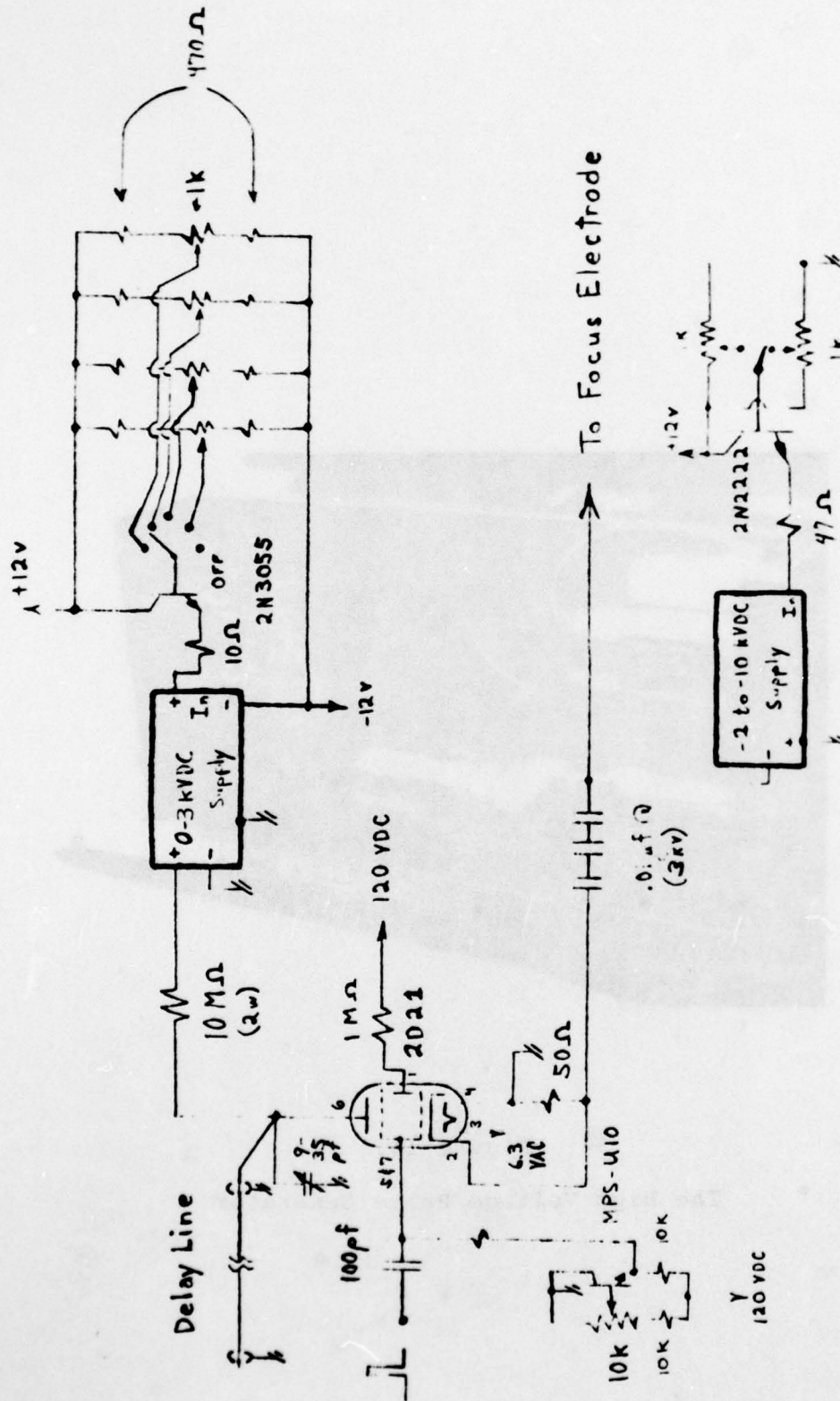


Figure 13. Schematic of the High Voltage Pulse Generator and the Focus Electrode Bias

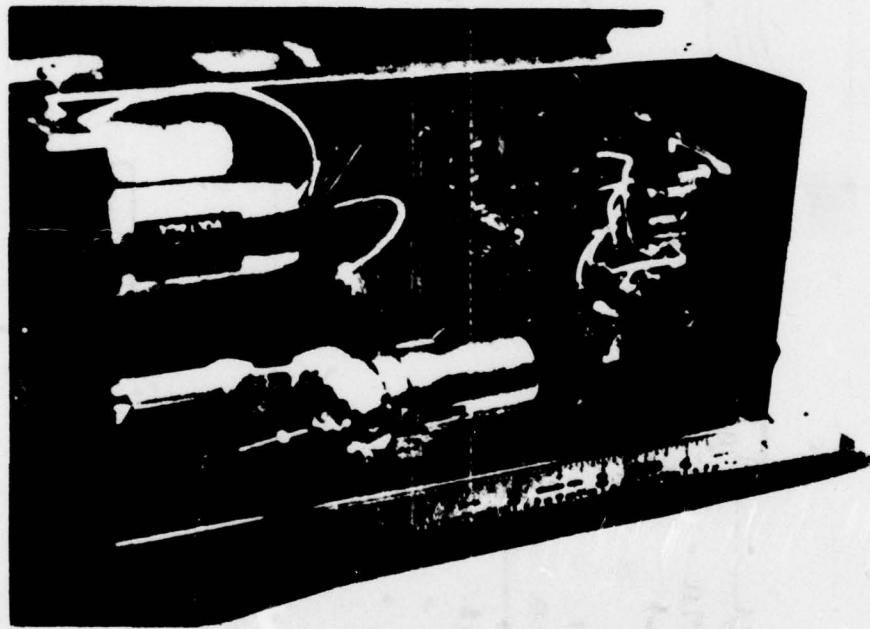
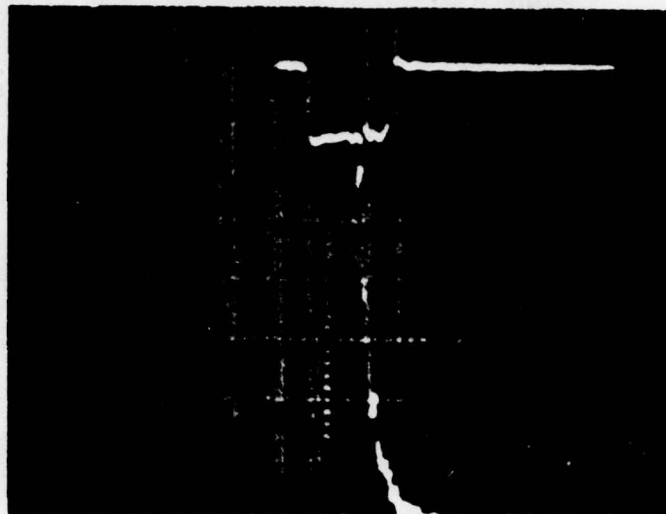
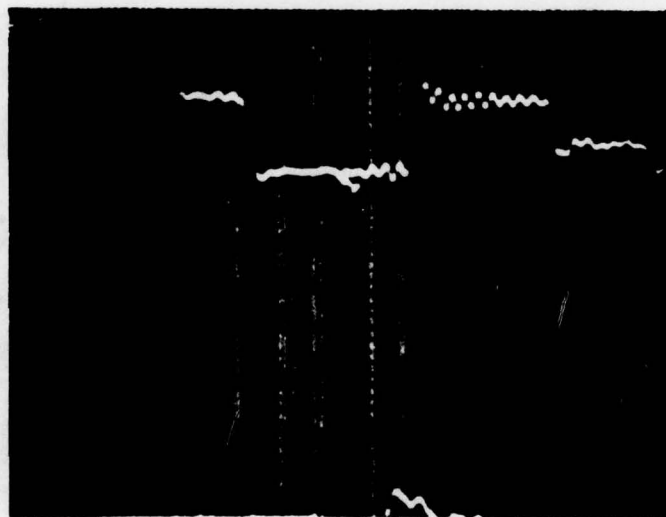


Figure 14.
The High Voltage Pulse Generator



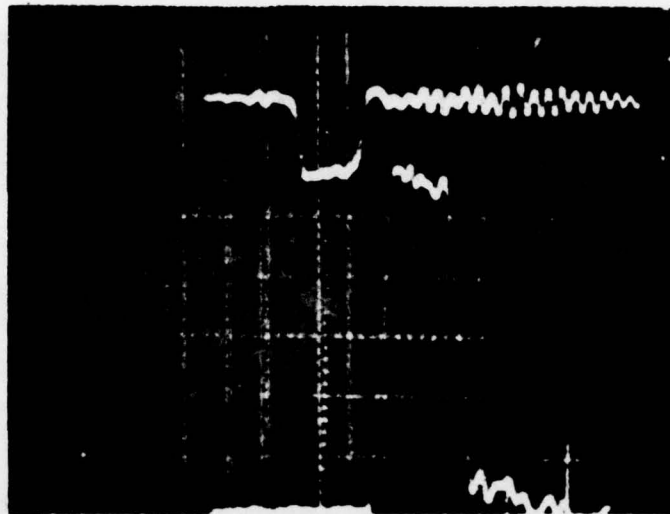
a) 10 nsec Pulse Horizontal Scale is 100 nsec/div.



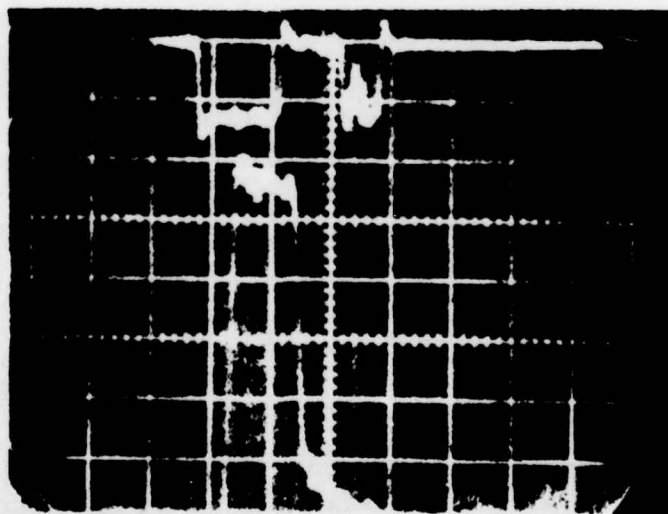
b) 25 nsec Pulse Horizontal Scale is 50 nsec/div.

Figure 15.

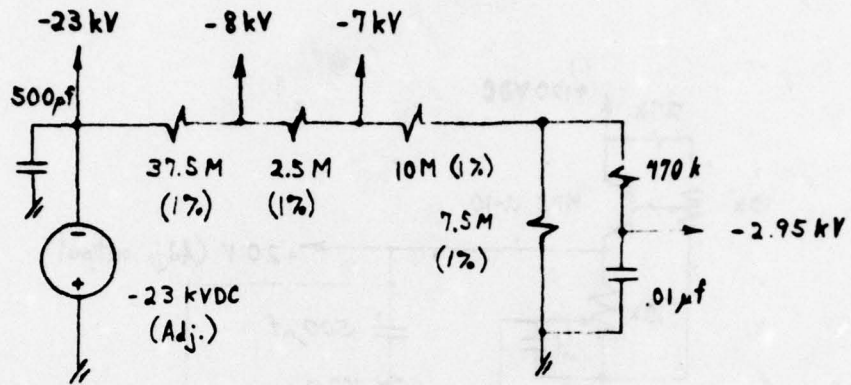
Output Pulses from High Voltage Pulse Unit
(Vertical Scales—Upper, 20 v/div;
Lower, 200 v/div.)



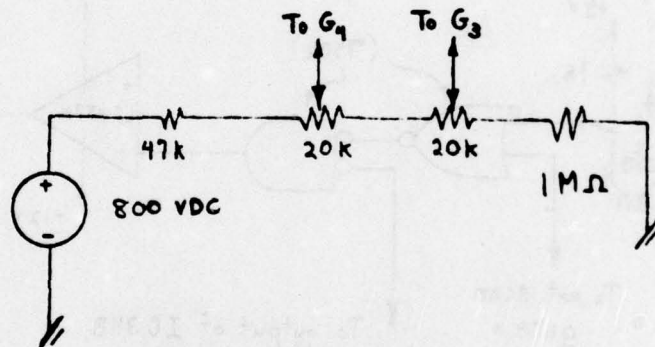
c) 50 nsec Pulse Horizontal scale is 50 nsec/div.



d) 100 nsec Pulse Horizontal Scale is 100 nsec/div.



a) Imaging Section



b) Scanning Section

Figure 16.

High Voltage Biasing

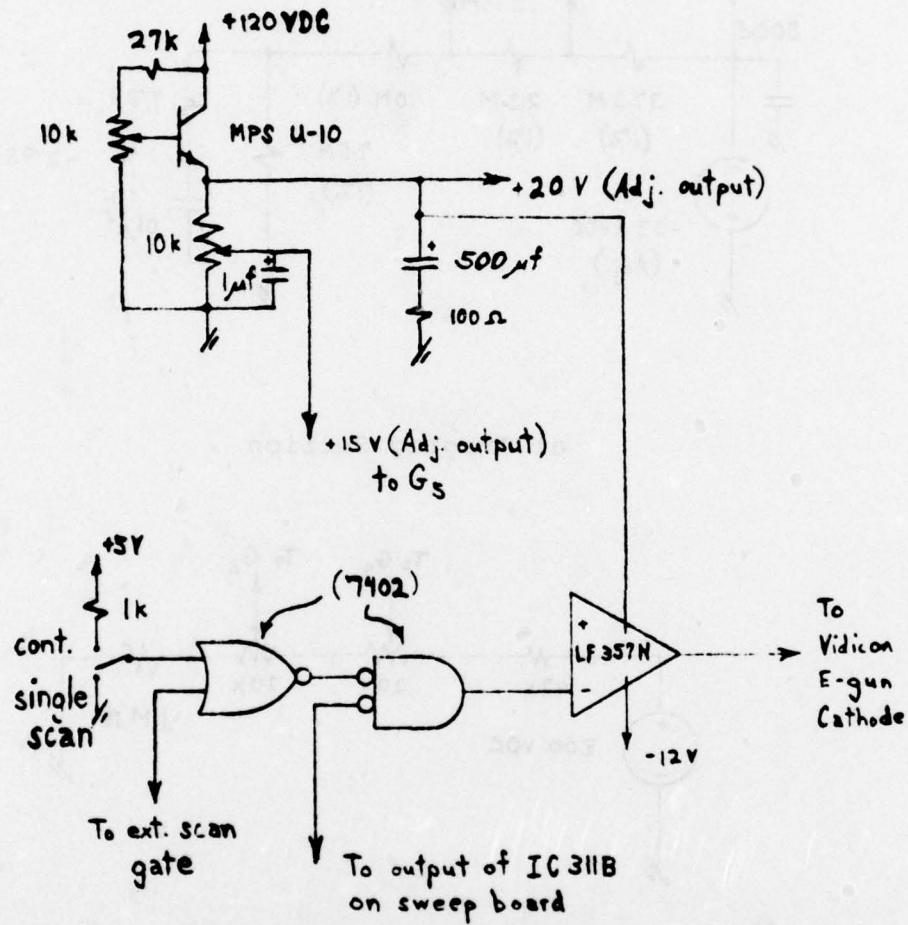


Figure 17.

Cathode Blanker Circuit

Another circuit added to the system is a cathode blanking board. This board applied the 30 Volt positive signal to turn off the reading beam for the tube. External control of this function is desirable, so interfacing with a storage system or some external device is accomplished with a TTL chip. The LM 357 op amp is used then to turn the beam on and off. The voltages required to run this system are generated on-board. Figure 17 is a schematic of the cathode blanker board. It includes a connection to the sweep board which shuts off the beam when either of the deflection supplies stops for some reason.

Figure 18 is the alignment coil drivers, designed to allow ± 70 ma to flow through each of the alignment coils. This is the last additional circuit required to make the tube operate properly.

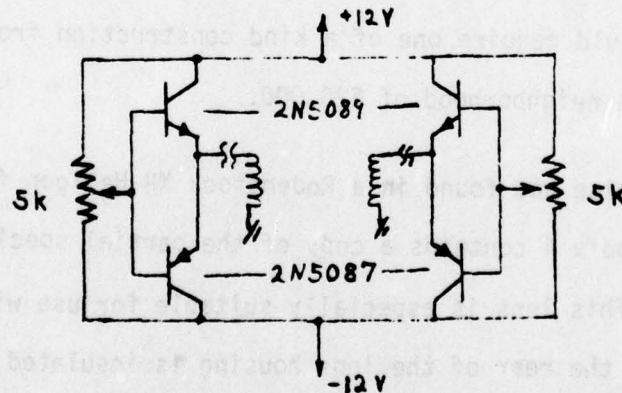


Figure 18. Alignment Drivers.

4.3 Optics for the Detector

It is necessary to collect as much light off of the window as possible and focus it as an image on the faceplate of the tube. This involves getting the objective portion of the optical system as close to the window as possible. The objective must be wide enough to cover the entire width of the window. The focused image must then fit on the 30x40 mm intensifier faceplate. Last of all, the lens must have a large aperture, i.e. it must have a low f number.

Using simple thin lens formulas, which actually do not apply specifically in this case, rough estimates of lens requirements were obtained. A lens of $f = .5$ with a 30 mm focal length was desired and thus searched for. After numerous optical products were investigated and ultimately discarded, it was determined that a lens of such abnormal specifications could not be obtained within budgetary limits. Such a lens system would require one of a kind construction from special glasses costing in the neighborhood of \$20,000.

A compromise was found in a Rodenstock XR-Heligon $f/.75$ -50 mm lens system. Appendix 4 contains a copy of the partial specifications for this system. This lens is especially suitable for use with the tube package since the rear of the lens housing is insulated against the photocathode high voltage. Disadvantages to the lens system include a short back focal length, a narrow angular field, and low spectral transmission (70%) at the wavelength at which the NE102 radiates.

A focusing system is also required. Since a lens is a device of a fixed aperture and focus, an externally movable lens mount was constructed. It enables the images to be focused by changing the objective-to-subject and imaging-to-focal plane distances. Figure 19 shows the simple arrangement that was used.

This optical system enables one to reduce a slit image by a factor of 2 with the middle 50% of the image in reasonably sharp focus. Better edge focusing is not attainable due to the narrow angular field of the lens.

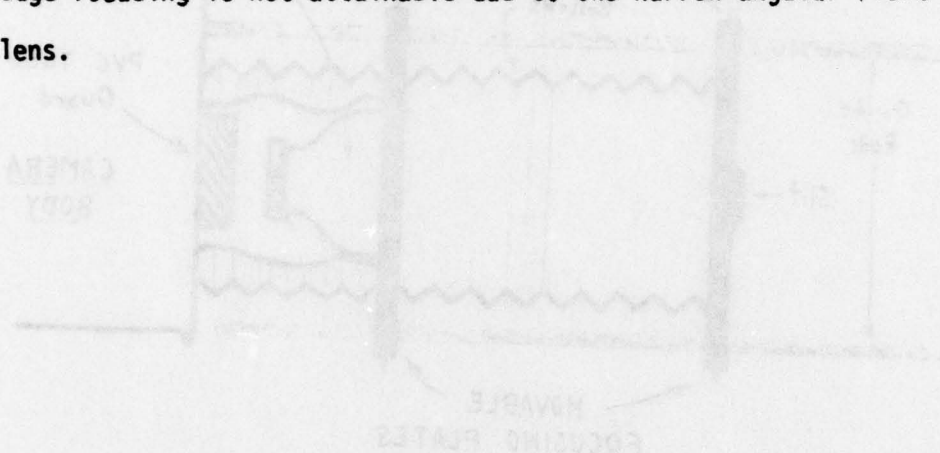


Figure 19
Diagram of Lens Focusing System

61

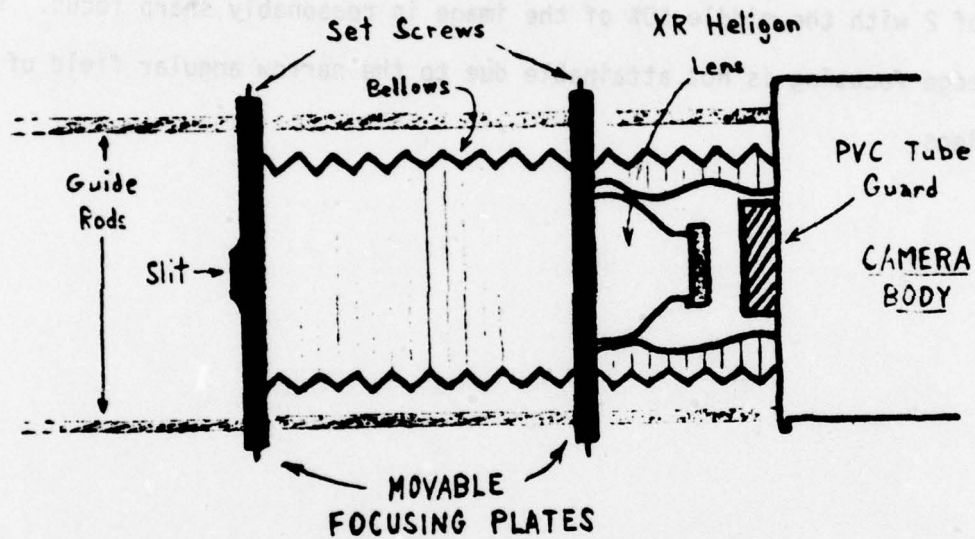


Figure 19.

Diagram of Lens Focusing System

CHAPTER V

THE DETECTION SYSTEM

One important part to a complete X-ray spectrometer system remains to be described. Since the pictures of X-ray spectra are generated (and erased) essentially in two video fields, a total duration of $1/30$ of a second, there must be some method of storing the video frame of interest.

During the construction of the high sensitivity vidicon camera, another project was also underway. It involved the design and construction of a video-disk storage, originally developed for use in pattern recognition. It is capable of storing a single video frame, provided the output of the video source is EIA RS-170 standard sync video. (28)

This system is essentially treated as a complete unit to go with the rest of the spectrometer. Figure 20 gives a block diagram of the entire X-ray spectrometer system.

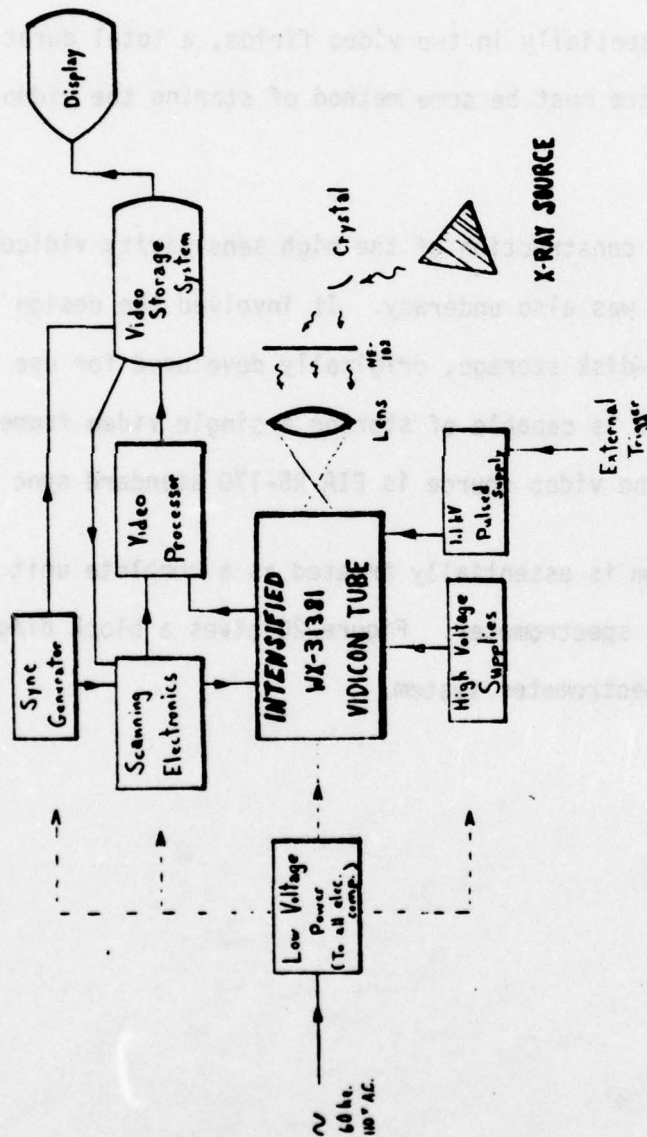


Figure 20. X-Ray Spectrometer System Block Diagram

CHAPTER VI

TESTS AND RESULTS

6.1 Introduction

There were two stages involved in the testing of the camera head and the results of these required a third test. The first two tests required the construction and calibration of light sources for the camera to detect. The camera was then tested in a steady state mode. This allowed the adjustment of all the standard video components and the video output signal. The imaging system was also checked and adjusted at this stage. Afterwards, when the steady state tests were deemed satisfactory, testing in the pulsed mode began. This chapter is a description of these tests and their results.

6.2 Steady State Testing

For this procedure, a light box was constructed from 1/4" aluminum plate. It was used in two different ways. First, it was used to provide a uniform illumination level for the entire photocathode of the imaging tube. This test was performed in order to see if the basic un-adjusted system was sensitive to light. After this test was completed, the light box was refitted to simulate a spectrometer scintillation window so that the camera could be adjusted for optimum resolution.

Figure 21 is a sketch of the light box. The light source within the box was a green LED with a series load resistor of $1k\Omega$. A variable voltage power supply enabled the radiant output of the LED to be varied

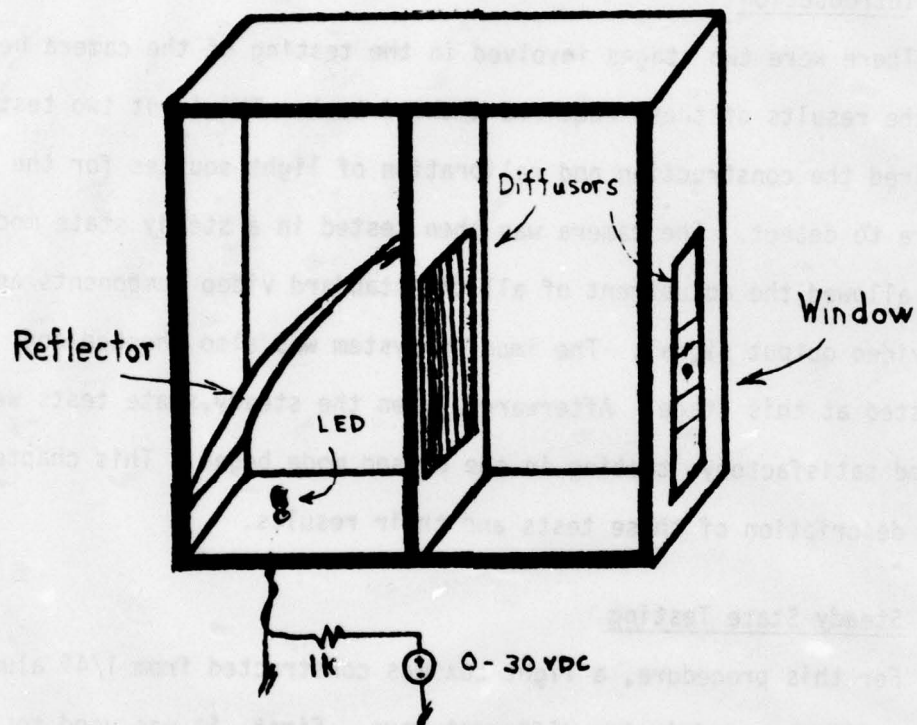


Figure 21.

Sketch of Light Box Used in Steady State
Testing

from zero to approximately 300 microwatts. A very large percentage of this light is absorbed in the box by the walls and the reflection and diffusion screens. Visual estimates of the light levels produced at the faceplate of the tube were in the range of from 10^{-5} to 10^{-3} foot candles.

Figure 22 is a photograph of the test stand and monitor for the focused testing stage. The dark circle on the monitor is a dot on the simulated window inside the light box. Resolution of much more detailed images is possible but do not show well photographically. (Better techniques will be required for a system which yields detailed X-ray spectra). From other test patterns, resolutions of >3 lines/mm were obtained.

The slit image was placed on a slight diagonal across the tube faceplate because any noise in the video system tends to run horizontally and vertically across the screen. The diagonal image may contain some low level fine structure and detail which is then more easily separated from this noise.

6.3 Pulsed Testing

The second critical testing point arrived after satisfactory results were obtained in the steady state tests. The pulsed mode operational tests required the calibration of a light source which gave outputs in the range from 1 to 1000 ft. candles. This source would then illuminate a simulated window with test markings on it.

Ordinary room light is in the range of from 1 to 100 ft. candles,

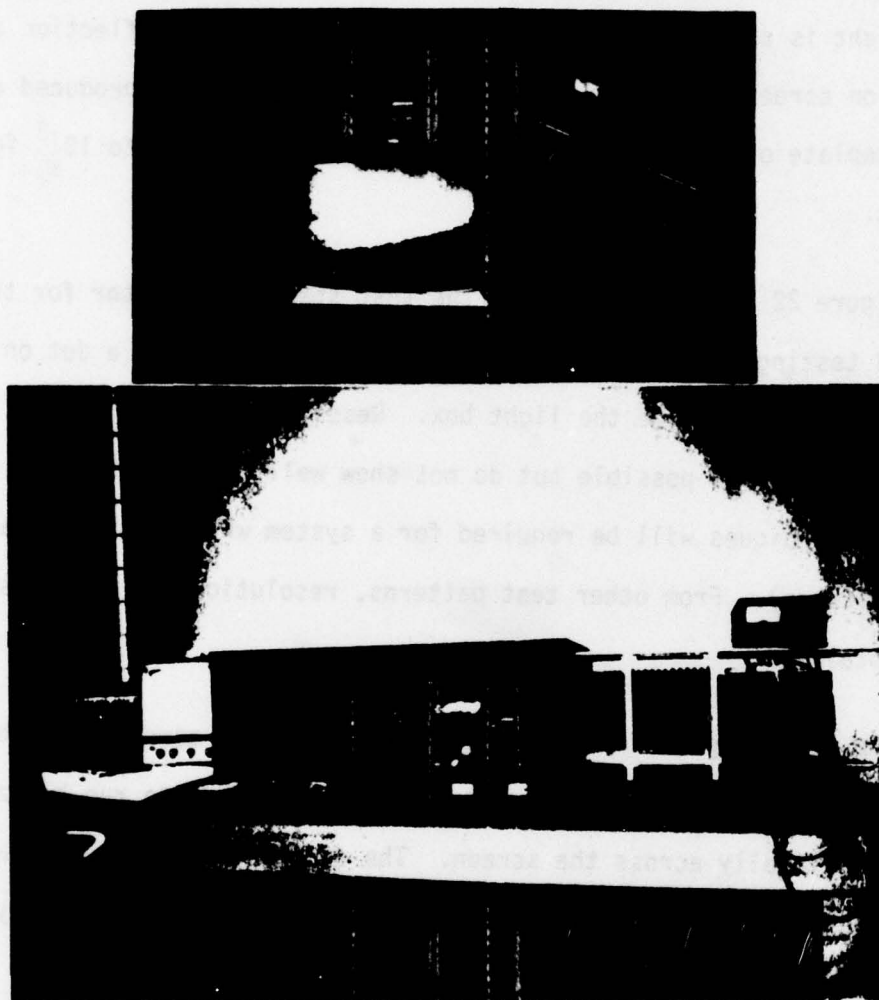
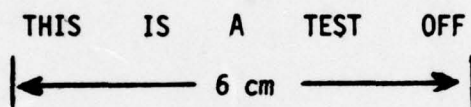


Figure 22.

The Steady State Test Setup

so an incandescent light was capable of providing the range of light levels required. A diagram and calibration table of the source used in the pulsed mode tests is given in Figure 23. Light levels directly behind the paper window were measured with a GE 213 light level meter, capable of giving readings from 5 to 2000 foot candles.

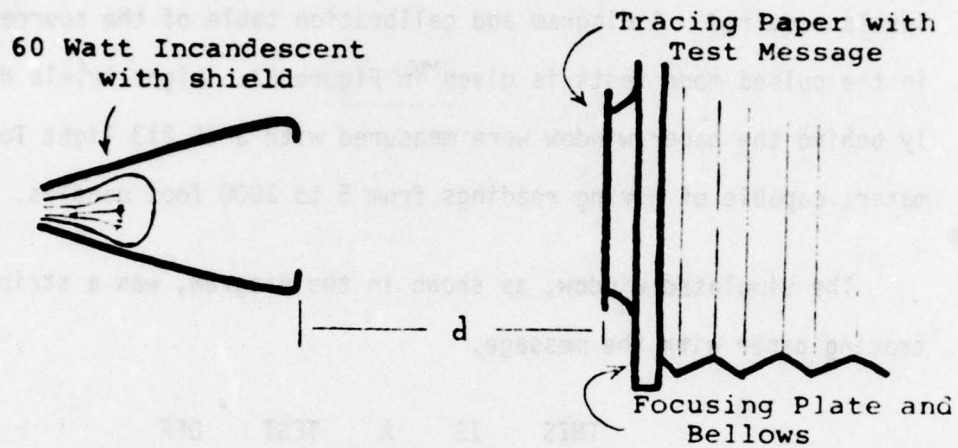
The simulated window, as shown in the diagram, was a strip of tracing paper with the message,



printed on it using dry transfer letters. It was attached to the slit opening on the focusing plate (see Figure 21). Proper operation of the camera in the pulsed mode should then yield single frame images of the test message. These images, incidentally, were obtained during steady state testing with essentially the middle 50% of the message in focus (see Section 4.3).

A block diagram of the pulse mode testing scheme is given in Figure 24. Pulsed testing began with $d = 24"$ (see Figure 23) and t_e set at $100\mu\text{sec}$. This should yield an effective light level at the tube faceplate of approximately 10^{-4} ft. candles. This is enough light to yield a resolvable image.

However, a resolvable image was not obtained. This occurred for two reasons. First, the imaging section appeared to introduce a great



d (in.)	Light Level at Slit (ft. c.)
1	900
3	500
5	280
8	150
10	110
12	80
15	50
17	40
19	30
23	20
28	15
34	10
43	5

Figure 23.

Diagram and Table of Light Source for Pulsed
Mode Testing

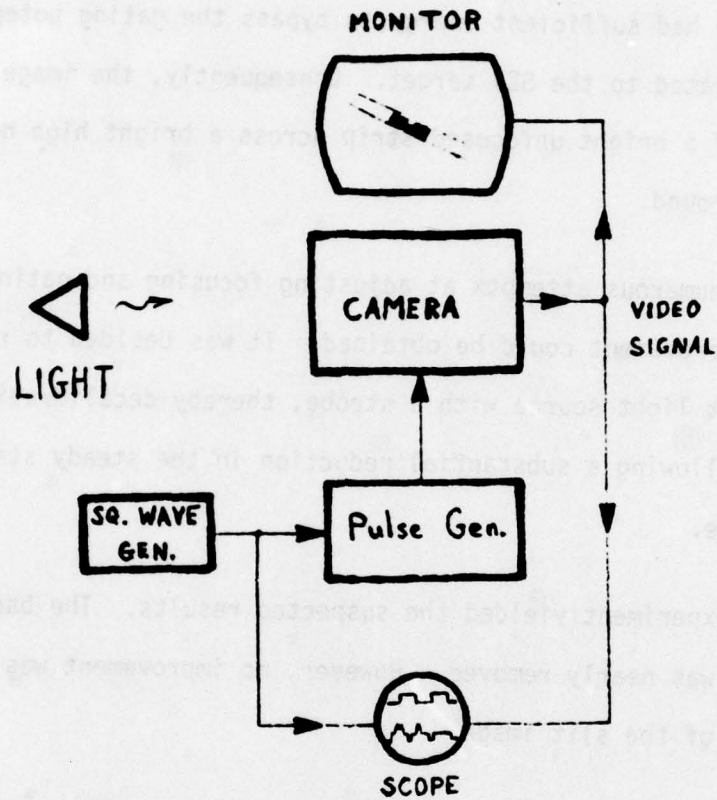


Figure 24.

Pulsed Mode Test Setup

deal of distortion in the form of defocusing. Secondly, the gating of the tube was not complete. Some photoelectrons off of the vidicon's photocathode had sufficient energy to bypass the gating potential and were accelerated to the SEV target. Consequently, the image obtained consisted of a bright unfocused strip across a bright high noise steady state background.

After numerous attempts at adjusting focusing and gating voltages, no image improvement could be obtained. It was decided to replace the incandescent light source with a strobe, thereby decalibrating the test setup but allowing a substantial reduction in the steady state background noise.

This experiment yielded the suspected results. The background brightness was nearly removed. However, no improvement was made in resolution of the slit image.

The slit was then taped in order to see if larger areas of light and dark could be resolved. Block tape was used to form an image which was a thick U-shape with the center of the U being a 3 mm square. This should have been easier to resolve than the submillimeter dry transfer letters.

Again, a focused image was unobtainable. The 3 mm square of light was visible on the monitor screen but only as an unresolved spot.

At this point, the author again consulted with the Westinghouse

Electron Tube Division. (29) Calculations on their part revealed a problem with the photocathode sheet resistance.

This is an unspecified value, in general, for the SEC vidicon tubes. For these tubes, however, it falls in the vicinity of 100k - 1000k Ω per square. Westinghouse calculations showed that, even assuming the optimistic value of 100k Ω /sq., a voltage profile with a magnitude of approximately 50 volts will fall across the tube photocathode when illuminated with a 10 to 20 ft. candle image. This is sufficient to cause image defocusing. Also, note that the profile magnitude could be up to ten times worse.

These calculations further revealed that the tube probably could not be gated at frame widths (t_e) less than 1 to 10 μ sec. This would avoid the above described effects of photocathode saturation.

Westinghouse further stated that SEC vidicons could be constructed, on a one by one basis, which would have lower photocathode sheet resistances. This could be accomplished by depositing a very thin layer of metal within the structure of the photocathode while it is under construction. (Westinghouse stated that it had done such work under contract about 10 years ago). This process could reduce the photocathode sheet resistance to <1000 Ω per square. However, the process could not be done to an existing tube.

This essentially halted the project. Budgetary and time allowances did not permit the consideration of rebuilding the camera

around a modified tube. It was decided at this point to do two things. First, institute another literature search, this one by the author, to make design recommendations to the project sponsor for rebuilding of the project. Secondly, a third experiment using the present tube in its integrating and storage mode would be run.

6.4 Integrating and Storage Mode Operation

This third experiment was attempted because it was thought the tube in the camera head had the capability to integrate low level signals for long periods of time (on the order of a minute) This would allow using the X-ray spectrometer in its steady state mode with the electron beam as its source. The detector could then integrate the output of the window for many seconds and then send an X-ray spectrum to the video-disk storage unit.

In general, the SEC tubes are manufactured such that the dark noise current off of the photocathode will give acceptable signal-to-noise levels so that integration periods of up to five seconds are possible. (30) Selected tubes are capable of yielding integration periods of up to thirty minutes. Storage times are generally several hours with the photocathode voltage turned off. (23)

This experiment, then, used the entire X-ray spectrometer system shown in Figure 20 with the X-ray source being the electron gun. According to Table 1, this should yield window illumination levels of

10^{-8} ft. candles. This is roughly equivalent to the background photon shot noise found in non-select tubes. (30) Thus it is first necessary to run the experiment with the electron beam turned off to see how long the tube can integrate without generating a large amount of background signal.

This experiment was tried. Since the tube was not specified for long integration capability, it is not surprising that after integration periods of from 5 to 10 seconds, background flash was deemed to be too bright to allow integration of the signal from the spectrometer.

CHAPTER VII

CONCLUSIONS AND WORK TO BE DONE

7.1 Conclusions Based on Literature Search

It is apparent that minor modifications to the camera head will not correct the problems due to the high photocathode sheet resistance. A subsequent literature search has shown that the distortion is definitely due to this effect. (31,32,33) Also shown in this search is that a reduction of the photocathode sheet resistance will solve the problem.

Westinghouse has stated that such special tubes can be constructed by them at their laboratories. (29) If desired, a package of the same form (WX-31381 plus intensifier) can be made. It is important to note that both the intensifier and the tube are subject to the same saturation effects. Therefore, both devices must incorporate low resistance photocathodes.

Bradley noted that satisfactory sub-nanosecond frame rates are obtained with photocathodes having sheet resistances of $10\Omega/\text{sq.}$ (31) Therefore, for the required 10 nanosecond frames for the X-ray spectrometer system, values of $1\text{K}\Omega/\text{sq.}$ should be satisfactory. This also allows the imbedded metal within the photocathode to be made thin enough so that the photocathode transmission is essentially unaffected. (29)

The rest of the circuitry involved in the camera head performed

satisfactorily. Thus, that design may be used with only minor convenience modifications. The operations manual will contain a full schematic description of the camera head.

7.2 Work to be Done

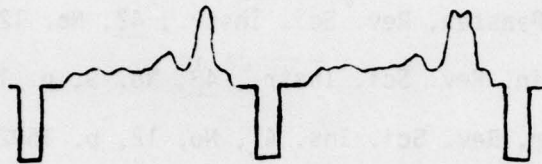
Again, the first thing which is to be done is the composition of an operations manual and electrical description for the camera head. Simultaneously, a refitting or reconstruction of the camera head by the project sponsor may also be done. When completed, testing may be resumed at the point where it was left off.

If the present system is not to be refitted, it may be converted to a fast frame ($\geq 10\mu\text{sec}$) low light level camera so that when used in conjunction with the video storage system, it may be used without further major modifications. The only modification necessary is an external connection to a device which is capable of generating the necessary 1.1 kV, $\geq 10\mu\text{sec}$ gating pulses.

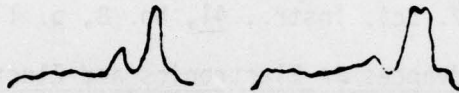
A total redesign of the detector around a silicon diode vidicon is also possible. Recent designs of such systems involve taking 5 μsec frames from the output of an X-ray spectrometer. (34) The output of such a device is not an image, however. Rather, it is an oscilloscope trace showing individual diodes charging and discharging.

A variation of this concept may be applied to our design. If the slit image is placed horizontally across the screen, the individual

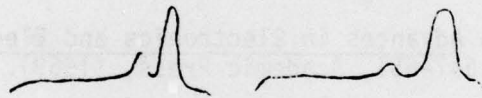
horizontal traces of the spectrum may be processed. For example, several lines may be taken, have noise removed from them, and then they could be added together to provide an enhanced trace which showed the details of the spectra. (See Figure 25).



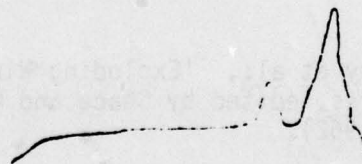
TWO HORIZONTAL LINES



REMOVE SYNC



PROCESS TO REMOVE HIGH
FREQUENCY NOISE



ADD LINES AND
RECONSTRUCT THE
SPECTRUM

Figure 25.

Illustration of How Horizontal Scan Lines
Could Be Processed

REFERENCES

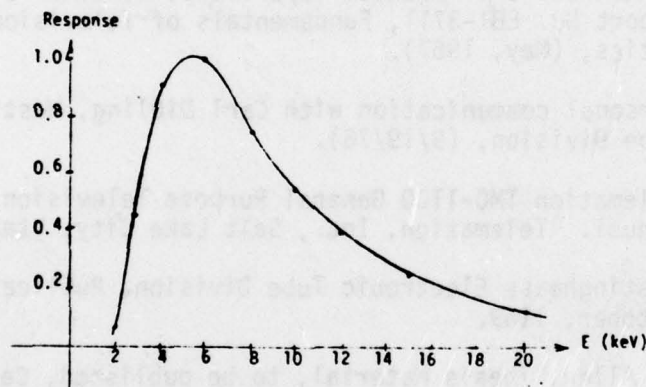
- 1) H. L. L. van Paassen, *Rev. Sci. Instr.*, 42, No. 12, p. 1823, (1971).
- 2) M. J. Bernstein, *Rev. Sci. Instr.*, 43, No. 9, p. 1323, (1972).
- 3) J. D. Strachar, *Rev. Sci. Ins.* 47, No. 12, p. 1592, (1976).
- 4) N. J. Peacock, M. G. Hobby, and P. D. Morgan, IAEA Conference Paper CN-28/D3, Madison, Wisconsin, (1971).
- 5) L. S. Birks, *Rev. Sci. Instr.*, 41, No. 8, p. 1129, (1970).
- 6) B. Driard, in *Advances in Electronics and Electron Physics*, Vol. 28B, pp. 931-937, Academic Press, (1969).
- 7) M. Blamoutier, in *Advances in Electronics and Electron Physics*, Vol. 28A, pp. 273-280, Academic Press, (1969).
- 8) W. Herstel, in *Advances in Electronics and Electron Physics*, Vol. 28B, pp. 647-651, Academic Press, (1969).
- 9) B. Combée, P. J. M. Botden, and W. Küh1, in *Photoelectronic Imaging Devices*, edited by L. M. Biberman and S. Nudelman, Vol. 2, Chapter 7, Plenum Press, (1971).
- 10) M. J. Bernstein and F. Hai, *Rev. Sci. Instrum.*, 41, No. 12, p. 1843, (1970).
- 11) I. M. Vitkovitsky et al., 'Exploding Wires as a Source of X-Rays,' in *Exploding Wires*, edited by Chace and Moore, Vol. 2, pp. 87-96, Plenum Press, (1962).
- 12) S. K. Händel, B. Stenerhag, I. Holmström, *Nature*, Vol. 209, No. 5029, pp. 1227-1228, (March 19, 1966).
- 13) J. Holmström, S. K. Händel, B. Stenerhag, *Journal of Applied Physics*, 39, No. 7, p. 2998, (1968).
- 14) A. E. Vlastos, *Journal of Applied Physics*, 44, No. 1, p. 106, (1973). See also references 12 and 13.
- 15) See references 12 and 13.
- 16) Project Proposal submitted to NSF, 'Development of a Nanosecond Resolution X-Ray Detector for an X-Ray Spectrometer,' Carlton E. Speck, Case Western Reserve University, Cleveland, Ohio, (1974).

- 17) Nuclear Enterprises NE102 Plastic Scintillator.
- 18) B. Stenerhag, S. K. Händel, and B. Göhle, *Journal of Applied Physics*, 42, No. 5, p. 1876, (1971).
- 19) See reference 18, p. 1881, Fig. 7.
- 20) R. H. Huddleston, S. Howard, ed., Plasma Diagnostic Techniques, Academic Press, New York & London, (1965), pp. 582-583.
- 21) A. J. Meyerott, et al., *J. Sci. Instr.*, 43, No. 1, pp. 93-96, (1966).
- 22) J. H. Adlam, et al., *J. Sci. Instr.*, 43, No. 1, pp. 93-96, (1966).
- 23) Westinghouse Electronic Tube Division, Publication TD 86-817, March, 1968.
- 24) For a general introduction to television signals and for the terms involved, see reference 23 and also: General Electric Visual Communications Products Department, Consumer Electronics Division, Report No. EBI-3711, *Fundamentals of Television and Essentials of Optics*, (May, 1967).
- 25) Personal communication with Carl Dibling, Westinghouse Electronic Tube Division, (9/19/76).
- 26) Telemation TMC-1100 General Purpose Television Camera Instruction Manual. Telemation, Inc., Salt Lake City, Utah, (1973).
- 27) Westinghouse Electronic Tube Division, Publication TD 86-823, October, 1969.
- 28) J. Allen, Thesis Material, to be published, Case Western Reserve University, Cleveland, Ohio.
- 29) Private telephone communication with Joseph Malanoski, Westinghouse Electron Tube Division, (5/22-5/25, 1978).
- 30) Westinghouse Electronic Tube Division, Publication No. TD 86-827, p. 6, September, 1968.
- 31) D. J. Bradley, *Applied Optics*, 8, No. 10, pp. 1959-1960, (1969).
- 32) A. J. Lieber, H. D. Sutphin, *Rev. Sci. Instr.*, 42, No. 11, p. 1663, (1969).
- 33) M. Y. Schelev, et al., *Applied Physics Letters*, 18, No. 8, p. 354, (1971).
- 34) D. R. Ciarla, *IEEE Transactions on Electron Devices*, ED-20, No. 4, p. 362, (1973).

APPENDIX 1

RESPONSE OF NE 102 SCINTILLATOR TO UNIFORM NUMBER OF PHOTONS

(dN/dE is Constant) INCIDENT



Relative number of visible photons produced per
x-ray of energy E. Data normalized on response
at 6KeV.

THIS PAGE IS BEST QUALITY PRACTICABLE
FROM COPY FURNISHED TO DDQ

APPENDIX 2

SPECIFICATIONS FOR THE COUPLED TUBE PACKAGE

COUPLED PACKAGE TUBE PERFORMANCE

Tube performance given for 4 x 3 Raster 525 TVL
@ 1/30 sec. frame time, normal scan

WIDE ANGLE TUBE SENSITIVITY

L.L. = 1×10^{-4} fc 3400 μ A/ft

VISIBLE RESOLUTION - W.A. CENTER 550 TVL/RT HT
80% EDGE 500 TVL/RT HT
EDGE FOCUS $Eg_3 = 753$ V

DISCERNIBLE RESOLUTION - W.A.

L.L. = 9.14×10^{-8} fc 100 TVL/RT HT
L.L. = 5.33×10^{-5} fc 550 TVL/RT HT
N.A. 900 TVL/RT HT

BLEMISHES

See Quality Photo

VOLTAGES & CURRENTS

Vpc = -23 kv	Photocathode of I1
Vsec = - 8 kv	Anode of I1 & photocathode of SEC
Vff = - 7.5 kv	SEC Focus Electrode
Vzz = - 7.0 kv	SEC Zoom Electrode
Vce = - 2.95 kv	SEC Corrector Electrode
Va = 0	SEC Anode & Sec Anode Flange

COUPLED PACKAGE TUBE PERFORMANCE (CONTINUED)

GUN VOLTAGES

 $E_{g1} = -54.6 \text{ V}$ For $\pm \text{sig} = 400 \text{ mA}$ $E_{g2} = 300 \text{ V}$ $E_{g3} = 726 \text{ V}$ $E_{g4} = 744 \text{ V}$ $E_{g5} = 15 \text{ V} \equiv \text{Suppressor Mesh}$ $I_H = +42 \text{ mA}$ $I_v = 44 \text{ mA}$ $I_{g2} = .30 \text{ mA}$ @ $E_{g1} = -54.6 \text{ V}$

SQUARE WAYERESPONSE - W.A.

100 TVL/RT HT = 87%

 $I_B = 400 \text{ mA}$ $I_{\text{sig}} = 250 \text{ mA}$

200 TVL/RT HT = 68%

300 TVL/RT HT = 40%

400 TVL/RT HT = 28%

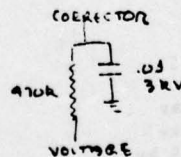
500 TVL/RT HT = 8%

SQUARE WAYERESPONSE - N.A.

See Photo

© Magnification = 2.0

NOTE: WX-31381BR and Varo image intensifier ground and polished within 1.5μ flatness. Both tubes coupled dry with aluminum clamping rings and lucite centering disc. Clamping screws torqued to 13 oz.-in. Corrector capacitor $\equiv .01 \text{ Mf}$ and $R = 470 \text{ K}$ connected to corrector and GD.



APPENDIX 3

This is listing of the corrections made to Telemation sweep board in order to make it compatible with the WX-31381 tube and its focus and deflection coils.

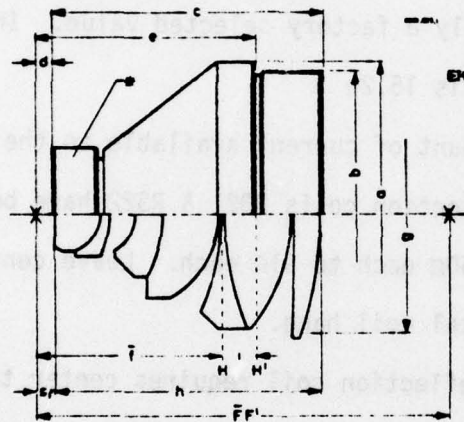
- 1) G_3 from tube connects to on-board 300V supply.
- 2) Output of IC 311B to Cathode Blanker Board.
- 3) R386 is normally a factory selected value. In this system it is 15.2Ω .
- 4) To increase amount of current available to the horizontal deflection coils R321 & R322 have been changed from 160Ω each to 91Ω each. Leave center top on horizontal coil hang.
- 5) The vertical deflection coil requires center top to be connected to middle of its parallel resistance to eliminate ringing. Therefore, replace R356 with 2 $3.3K\Omega$ resistors with an available center top.

Refer to the Telemation TMC-1100 instruction manual and to the forthcoming camera operations manual for the details and locations of these modifications.

APPENDIX 4

SPECIFICATIONS OF THE XR - HELIGON LENS

This lens has been computed especially for use with X-ray image intensifiers. It is being used as collimating lens in a tandem system with the purpose of transmitting the anode image from the image intensifier tube onto the cathode of a TV-taking tube or sensitive film.



ERCONA CORPORATION
3482 Merrick Road
Baltimore, N. Y. 11718
(516) 781-2770

Optical data:

Focal length ($-f$)	51.8 mm
Relative aperture	$f/0.75$
Angular field $2w$	16.6°
Image diameter $2y$	15.0 mm
Image scale β	$\infty : 1$
Corrected for range of wave lengths	450-650 nm
Back focus ($-s_p$) in air	5.2 mm
Nodal point separation i	11.2 mm
FF	114.9 mm
Thickness of screen glass of tube taken into account in correction	3.2 mm

Mechanical data:

Maximum diameter of mount (a)	85.0 mm
Diameter of front ring (b)	M 80 x 1
Total length (c)	ca 75 mm
Distance from end of mount to image in air (d)	ca 4.7 mm
Distance from seating face to image in air (e)	61.3 ± 0.5 mm
Free diameter of front lens element (g)	68.0 mm
Overall length of lens system (h)	73.8 mm
Weight	945 g
* The rear part of the mount is insulated against tube side high voltage.	

All indicated data were valid at the time of going to press. They are not binding since modifications may become necessary in the interest of further improvement which will then be incorporated without prior notice. Only the technical information which is being submitted together with our quotations may be considered binding.

The concept of substituting the "liner" for a SHIVA injection chamber by plasma injected from a subsidiary gun had been proposed a few years ago by R. W. K. (1). In order to test the feasibility of this idea, a series of investigations were performed in which plasmas produced by a coaxial gun of the linear type (2) was introduced in a container analogous

PART III

PLASMA INJECTION

for

A SHIVA MACHINE

by

O.K. MAWARDI AND A. FERENDECI

decided to study the behavior of the plasma injected through a coaxial gun in a first stage and to compare it with the behavior of the plasma as it escaped from two neighboring holes.

This report summarizes the results obtained and reports on the preliminary measurements of electron densities and on photographic observations of the plasma jet.

1. PLASMA FOR A SHIVA MACHINE

The required densities were found from the assumption that a ring of plasma was to be injected inside the injection chamber. The plasma was to be introduced through 80 holes, each 1 cm in diameter, and aligned on a circle of twenty centimeters in radius. The expansion chamber is approximately 1 m high. It is important, therefore, that the plasma will be uniform in the axial direction and would not recede during the filling time.

Now the characteristic radiation on the line is given by $I = \frac{1}{2} n^2 V$

Introduction

The concept of substituting the "liner" foil in SHIVA implosion chambers by plasma injected from a subsidiary gun had been proposed a few years ago by M. Wolfe.⁽¹⁾ In order to test the feasibility of this idea, a series of investigations were performed in which plasma produced by a coaxial gun of the Cheng type⁽²⁾ was to be introduced in a container analogous to the implosion chamber.

Because the plasma had to be injected through a number of circular holes whose centers were arranged on a circle, there was some concern on the influence of the non uniform distribution in the azimuthal direction of the plasma density. To evaluate the extent of this non-uniformity it was decided to study the behavior of the plasma as it is injected through a circular orifice in a flat plate and to compare it with the behavior of the plasma as it escapes from two neighboring holes.

This report summarizes the results obtained and reports on the preliminary measurements of electron densities and on photographic observations of the plasma jet.

Criteria for Plasma Densities

The required densities were found from the assumption that 1 mgm. of plasma was to be injected inside the implosion chamber. The plasma was to be introduced through 30 holes, each 1 cm in diameter, and aligned on a circle of twenty centimeters in radius. The explosion chamber is approximately 1 cm high. It is important, therefore, that the plasma will be uniform in the axial duration and would not recombine during the "filling" time.

Now the characteristic radiation cooling time is given by $\tau = \frac{m_e k T_e}{W}$

where W , the radiation power per unit volume, is contributed by the force-free transitions and force-bound transitions. Actually

$$W = W_{ff} + W_{fb}$$

$$= (1.52 \times 10^{-32}) m_e^2 T_e^{1/2} + (4.11 \times 10^{-31}) m_e^2 T_e^{-1/2} \text{ in watts/cm}^3$$

In the above relation m_e is the mass per cm^3 and T_e is in eV. The temperature thus falls like $T_e = T_{\text{initial}} (\exp - \frac{t}{\tau})$.

Now if we require $v_{th} = 0.1 v_{\text{directed}}$ in the implosion chamber and $v_{\text{direct.}} = 1 \text{ cm}/\mu\text{sec}$, then

$$v_{th} = \left(\frac{2T_e}{m_e} \right)^{1/2} = 0.1 v_{\text{direct.}} = 10^5 \text{ cm/sec.}$$

This defines

$$T_e = \frac{1}{2} m_e \times 10^{10} \\ = T_{\text{init.}} (\exp - \frac{t}{\tau})$$

Hence, for a given initial $T_{\text{init.}} \approx 10 \text{ eV}$, the time needed to allow the temperature to cool to $T_e \approx 3 \text{ eV}$ is of the order of $1 \mu\text{sec}$.

The mass m_e used above indicated that one would need a density of at least $10^{17}/\text{cm}^3$ (for Helium).

Summary of Diagnostics Performed

The SHIVA implosion chamber was simulated by two parallel plates. One of the plates had in it a hole 1 cm in diameter. In a subsequent experiment the perforated plate was replaced with one which had two holes.

The important parameters that were needed to be measured were: the directed velocity of the plasma prior to its impinging on the plate, its

velocity after its escaping through the orifice in the plate, the extent of divergence of the plasma jet as it leaves the plate and the density of the plasma in these various conditions.

The velocities of the plasma were inferred from an STL image converter camera used in a streaking mode. The divergence of the beam was directly seen from the STL camera used as a frame camera. The plasma density was measured by means of an Ashby-Jephcott⁽³⁾ laser interferometer used directly as developed by Ashby and Jephcott or as modified by Bekefi⁽⁴⁾. The first method is suited for the higher density range in which the interferometer yields several fringes, while the other is specially suited when one detects a fraction of a fringe.

Results

The beam velocity was observed to be approximately 5 cm/ μ secs. This higher velocity works to our advantage since the transit time of the plasma over a length equal to the height of the implosion chamber is much shorter than the recombination time of the plasma.

It was found also that it was important to electrically float the plate. When grounded, appreciable return currents flow to the ground. These currents, if asymmetric, cause the plasma beam to acquire a whipping motion.

Visual observation of the appearance of the plate revealed that the plate was seriously ablated, even after one experiment. It thus appeared that an appreciable amount of metal vapor is injected in the implosion chamber together with the plasma. Several fringes were detected on the interferometer, thus indicating that the electron density is quite high. In fact, we estimated it to be at least $5 \times 10^{17}/\text{cm}^3$ and more probably $10^{18}/\text{cm}^3$. The density of the ablatants is best found from the measurement of the intensity of radiation of the Aluminum (for an Al plate) or Copper line. Unfortunately,

these lines are very close to the He-Ne laser line so that narrow band interference filters are needed to differentiate these lines of each other. Since we did not have such filters in our laboratory, we estimated the ablatant density from the mass of material ablated. This estimate yielded the remarkable result that about 10 mgms appear to be entrained by the plasma.

The preliminary results described here show that plasma injection is most promising.

References

- (1) M. Wolfe. Private communication. Wolfe unfortunately never had an opportunity to test his idea since he died in an accident.
- (2) D.Y. Cheng: Bull. Am. Phys. Soc. 13, 1560 (1968).
- (3) D.E.T. Ashby et al: J. Appl. Phys. 36, 29 (1965).
- (4) E. Hooper and G. Bekefi: J. Appl. Phys. 37, 4083 (1966).

UNCLASSIFIED

SECURITY CLASSIFICATION OF THIS PAGE (When Data Entered)

REPORT DOCUMENTATION PAGE		READ INSTRUCTIONS BEFORE COMPLETING FORM
1. REPORT NUMBER AFOSR-TR- 78 - 1269	2. GOVT ACCESSION NO.	3. RECIPIENT'S CATALOG NUMBER
4. TITLE (and Subtitle) THEORY AND CONSTRUCTION OF TIME RESOLVED X-RAY SPECTROMETER		5. TYPE OF REPORT & PERIOD COVERED Final Report Jan. 31, 1975 to Jan. 31, 1978
7. AUTHOR(s) O.K. Mawardi, C. Speck, R. Vesel and A. Ferendeci		6. PERFORMING ORG. REPORT NUMBER
9. PERFORMING ORGANIZATION NAME AND ADDRESS Case Western Reserve University Cleveland, Ohio 44106		8. CONTRACT OR GRANT NUMBER(s) AFOSR-75-2806
11. CONTROLLING OFFICE NAME AND ADDRESS AFOSR/NP Bolling Air Force Base Bldg 410 Rm C219 Washington, D.C. 20332		10. PROGRAM ELEMENT, PROJECT, TASK AREA & WORK UNIT NUMBERS 611021 2301/A2
12. REPORT DATE August, 1978		13. NUMBER OF PAGES 92
14. MONITORING AGENCY NAME & ADDRESS (if different from Controlling Office)		15. SECURITY CLASS. (of this report) Unclassified
16. DISTRIBUTION STATEMENT (of this Report) Approved for Public Release: Distribution Unlimited		15a. DECLASSIFICATION/DOWNGRADING SCHEDULE
17. DISTRIBUTION STATEMENT (of the abstract entered in Block 20, if different from Report) This document has been approved for public release and sale; its distribution is unlimited.		
18. SUPPLEMENTARY NOTES		
19. KEY WORDS (Continue on reverse side if necessary and identify by block number) x-rays, Spectrometer, Storage Scheme, Plasma Injection		
20. ABSTRACT (Continue on reverse side if necessary and identify by block number) This report describes the essential characteristics of a time resolved x-ray spectrometer. The spectrometer uses a convex curved LiF crystal which diffracts the x-rays onto a plastic (NE 102) scintillator. The spectrometer is capable of analyzing spectra in the range of 4.2 KeV to 12.4 KeV. It can also time resolve the observed spectra to approximately 2.4 μsec. with a wavelength discrimination better than 4%. The report also contains the calculations, design and calibration of the associated electronics for the detection of the optical signal which appears at		

DD FORM 1 JAN 73 1473

EDITION OF 1 NOV 65 IS OBSOLETE

Unclassified.

SECURITY CLASSIFICATION OF THIS PAGE (When Data Entered)

Unclassified.

SECURITY CLASSIFICATION OF THIS PAGE(When Data Entered)

the plastic scintillator. A video storage system detects and stores the signal from the spectrometer. The unfolding of the x-ray spectra can then be performed at a much slower rate. The optical detector consists of a WX-31381 vidicon tube.

The last part of the report consists of an attempt at finding a procedure to inject plasma in the implosion chamber of a SHIVA device. The plasma is projected on to a perforated plate which shapes it into a jet. The incident plasma density is higher than $5 \times 10^{17} / \text{cm}^3$. The energetic plasma, however, causes the metal from the plate to be ablated and to be entrained by the jet into the implosion chamber. The ablatant easily doubles the density of the injected material.

SECURITY CLASSIFICATION OF THIS PAGE(When Data Entered)